INTERNATIONAL ATOMIC ENERGY AGENCY
UNITED NATIONS EDUCATIONAL, SCIENTIFIC AND CULTURAL ORGANIZATION

INTERNATIONAL CENTRE FOR THEORETICAL PHYSICS
34100 TRIESTE (ITALY) - P.O.B. 586 - MIRAMARE - STRADA COSTIERA 11 - TELEPHONE: 2240-1
CABLE: CENTRATOM - TELEX 460392-1

SMR/291 - 35

SPRING COLLEGE IN CONDENSED MATTER
ON
"THE INTERACTION OF ATOMS & MOLECULES WITH SOLID SURFACES"
(25 April - 17 June 1988)

STRUCTURE OF ADSORBATES
(Lectures I, II, III & IV)

David A. KING
Department of Chemistry
Cambridge University
Lensfield Road
Cambridge CB2 1ET
UK

STRUCTURE OF ADSORBATES.

DAVID KING
CAMBRIDGE UNIVERSITY
U.K.

I. 1. CLASSIFICATION OF ADSORBATE STRUCTURES.
1. TECHNIQUES: A SURVEY.

II. 1. SURFACE EXAFS.
2. CORE LEVEL SHIFT SPECTROSCOPY/ PHOTOELECTRON DIFFRACTION.

III. CASE HISTORIES.

IV 1. INTERACTIONS BETWEEN ADSPECIES
2. ORDER - DISORDER PHENOMENA
3. KINETIC - STRUCTURE RELATIONSHIPS.

CAMBRIDGE SURFACE SCIENCE.

CHEMISTRY

D. A. KING — EXPTL.: HREELS, RAIRS, ARUPS, ISS, LEED, SEXAFS, SCLS, BEAMS
R. M. LAMBERT — EXPTL: SURF. SCI. / CATALYSIS. XPS, UPS, TPD, PED; REACTIVE BEAMS
D. CLARY — THEOR.: DYNAMICS, ENERGY BROADENING
P. B. DAVIES — EXPTL: TUNABLE IR LASERS.
W. JONES — EXPTL: XRD, ZEOLITES, CATALYSIS
D. JEFFERSON — EXPTL: EL. MICR., ZEOL., CATALYSIS
T. RAYMENT — EXPTL: 2D XRD; XRD OF CATALYSTS

PHYSICS (CAVENDISH)

R. F. WILLIS — EXPTL: ARUPS, NEUT. DIFFR., SURF. MAGN., HE DIFFR., ETC.
W. ALLISON — EXPTL: He DIFF., BEAMS.
A. HOWIE — EXPTL: EL. MICROSCOPY, STM.
V. HEINE — THEOR.: EL. STRUCTURE, PHASE TRANSITIONS, SOLID [illegible], ETC.
R. NEEDS — THEOR.: EL. STRUCTURE, ETC.

ENGINEERING

M. WELLAND — EXPTL: STM, DEVICES.
N. KENNEY — EXPTL: HETEROGENEOUS CATALYSIS
L. GLADDEN — EXPTL: NMR OF CATALYSTS

MATERIALS AND EARTH SCIENCES

PUTNIS, SOMEKH, EVETTS — SURFACE ANALYSIS, LASER MICROPROBE ANALYSIS, ETC.

CHEMISORPTION - ON METALS.

MODELS OF CHEMISORPTION STRUCTURES:

CONTINUOUS SURFACE

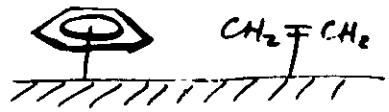

CHECKERBOARD

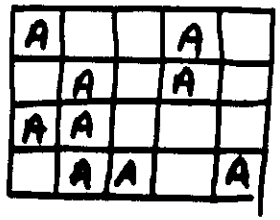

SURFACE COMPLEX

SPATIAL POSITIONS OF ATOMIC CONSTITUENTS OF A SOLID SURFACE ARE THE MOST FUNDAMENTAL PHYSICAL PARAMETERS CHARACTERISING THAT SURFACE.

ADSORBATE STRUCTURE

(i) CHECKERBOARD STRUCTURES.

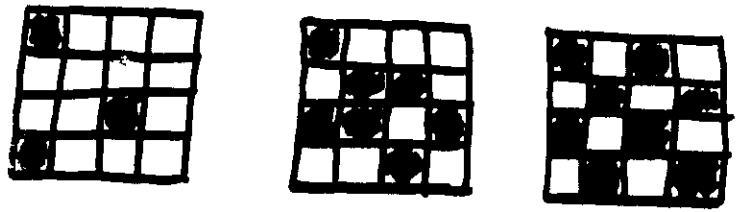

(ii) DISPLACIVE STRUCTURES

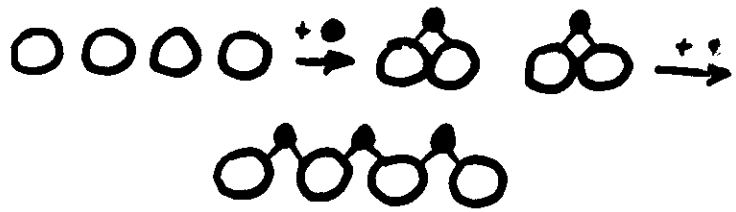

(iii) RECONSTRUCTION

CHECKERBOARD STRUCTURES

(i) SIMPLY RELATED

e.g. O on Ni{111}

p(2×2) $\begin{pmatrix} 2 & 0 \\ 0 & 2 \end{pmatrix}$

ANTICIPATE ORDER-DISORDER TRANSITIONS

(ii) RATIONALLY RELATED

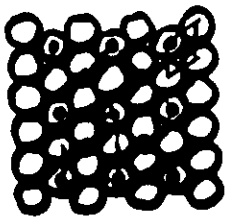

e.g. CO on Pt{111}

BRIDGE AND ON-TOP SITES

COINCIDENCE MESH

(iii) INCOMMENSURATE

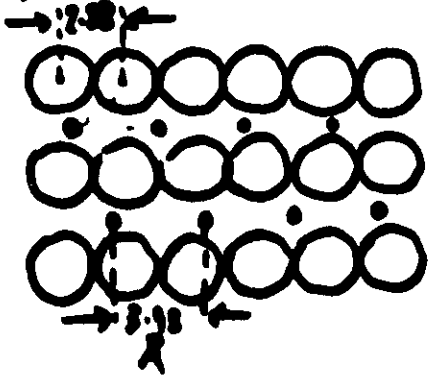

Cl on Ag{110}

UNIFORMLY INCOMMENSURATE MODEL

(BUT SEE LATER)

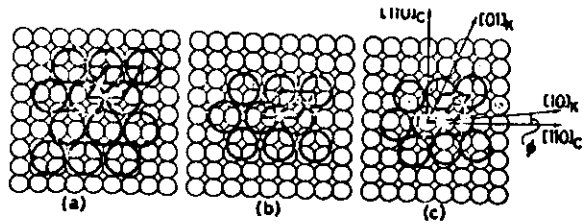

FIG. 1. Models for potassium monolayers (large circles) adsorbed on copper (001) surface (small c
C-1 structure, whose unit mesh is $\begin{pmatrix} 2 & 1 \\ 1 & 3 \end{pmatrix}$; (b) the C-2 structure, whose unit mesh is $\begin{pmatrix} 2 & 1 \\ 1 & 2 \end{pmatrix}$; (c) the incomm
ture. The [10] and [01] axes of the potassium monolayer are denoted by $[10]_K$ and $[01]_K$, and the [110]
of copper by $[110]_C$ and $[\bar{1}10]_C$.

Ann Arruga et al

1984

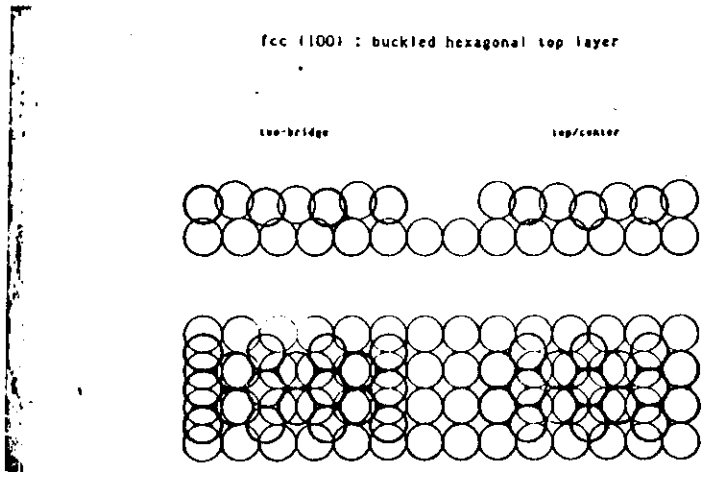

Van Hove et al 1984

STRUCTURAL TOOLS:

I. LOW ENERGY ELECTRON DIFFRACTION (LEED)

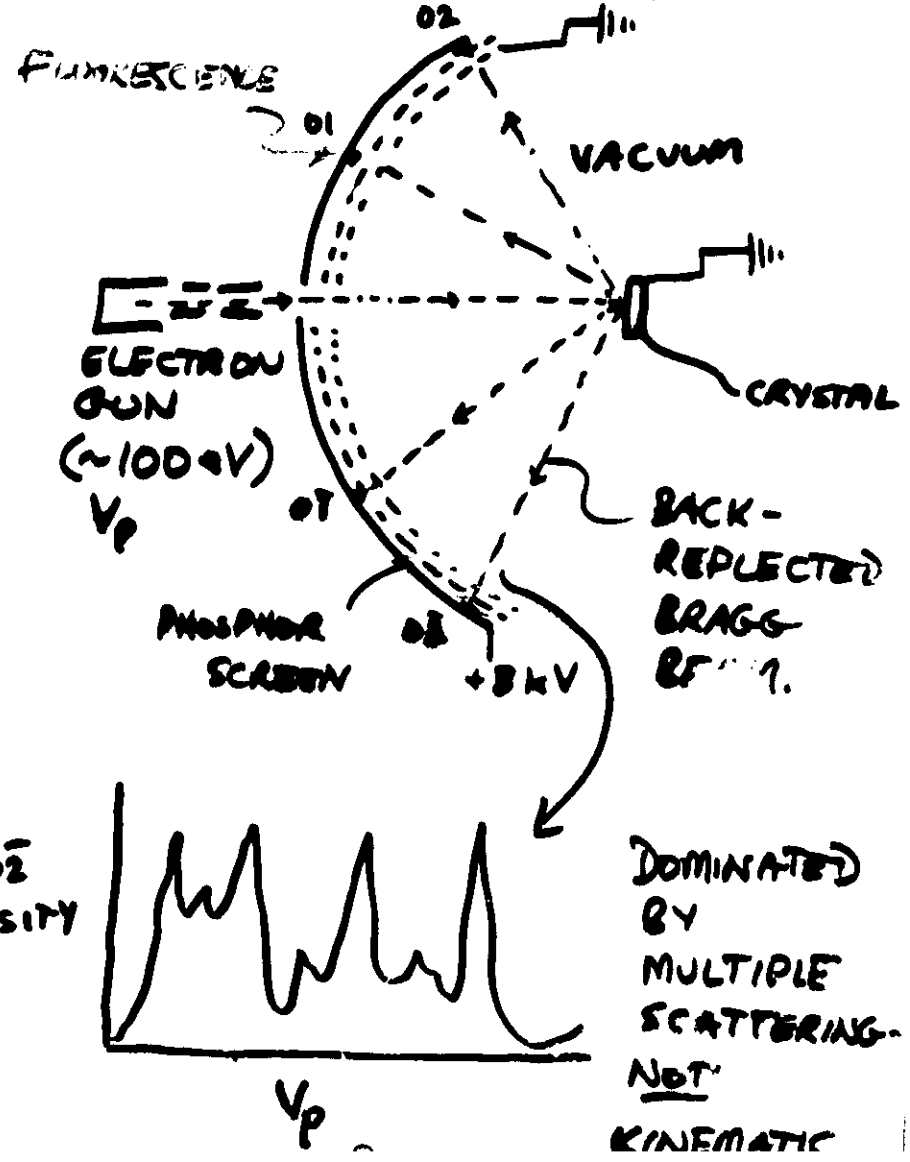

LEED Experiment.

Intensities measured by:

(i) A Faraday cup : absolute

(ii) Spot photometer reading of light intensity from screen.

(iii) Direct recording by a TV camera linked to computer : VIDEO - LEED.

(iv) Direct recording by resistive anode coupled to microchannel plate.

Fast data collection useful, sometimes essential.

Incidence angle must be accurate, at normal incidence clock symmetry.

Electron beam damage may be severe - ESD.

Experiment

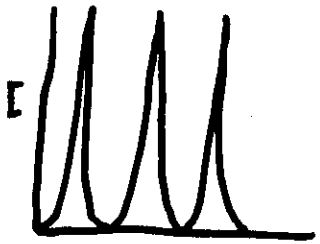

kinematic

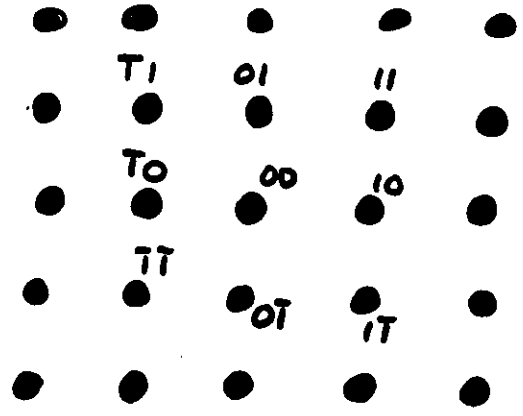

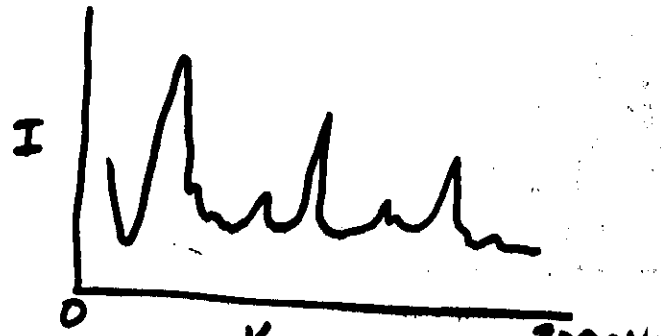

dynamical

12 experimental curves obtained, using
5 different beams
5 incidence angles.

$\theta = 0°$: 01, TT, $T\bar{1}$, $\bar{1}0$
$\theta = -5°$: $0\bar{1}$, 1T, $0\bar{1}$
$\theta = +9°$: 01, 00
$\theta = +14°$: 01, 00
$\theta = +18°$: 00

SYMMETRY ANALYSIS

eg. W{100} LEED PATTERN

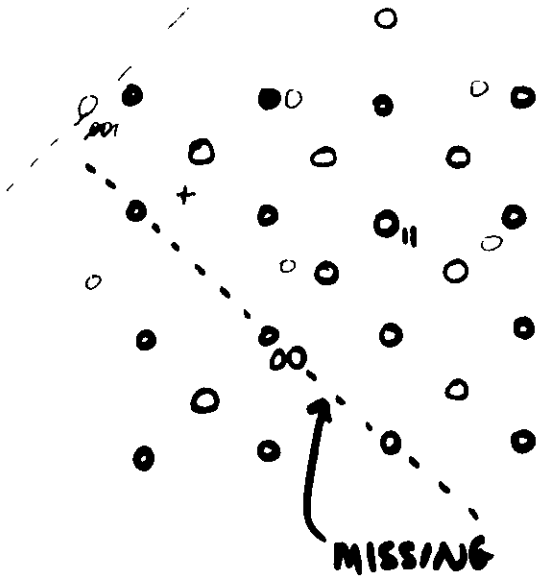

FROM STEPPED SURFACE — ONE ROTATIONAL SET OF DOMAINS MISSING

→ **GLIDELINE**

Low temperature phase of W{100}

Debe and King: symmetry analysis (1977)

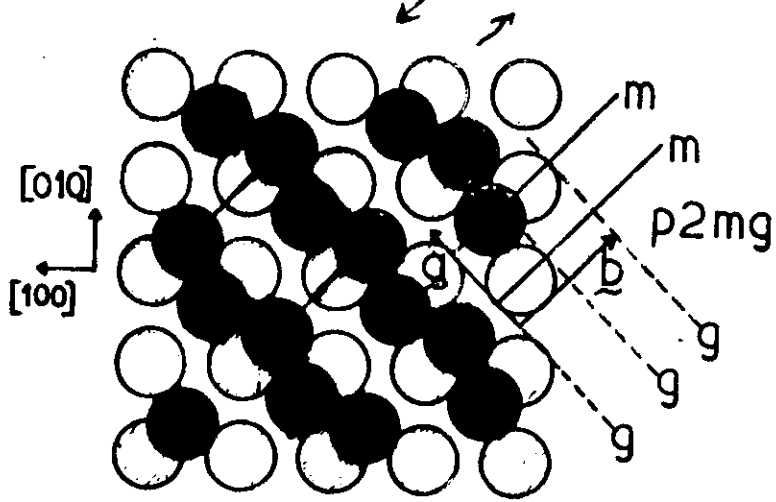

LEED I-V analyses:

(i) Barker, Estrup, Jona + Marcus. (1978)

(ii) Walker, Debe and King (1980)

6% contraction.
0.2 Å lateral shift.

Low temperature phase of W{100}

Debe and King: symmetry analysis (1977)

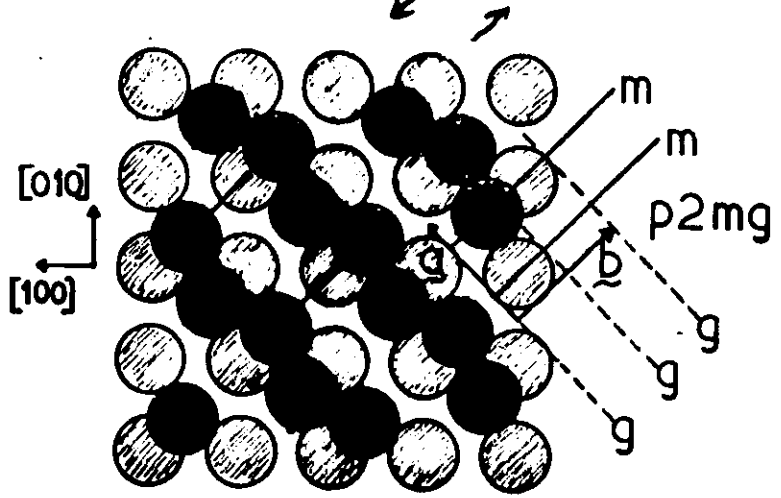

LEED I-V analyses:

(i) Barker, Estrup, Jona + Marcus. (1978)

(ii) Walker, Debe and King (1980)

6% contraction.
0.2 Å lateral shift.

CALCULATION OF DIFFRACTED INTENSITIES.

1. TRIAL STRUCTURE

2. CALCULATE NON-STRUCTURAL PARAMETERS
Phase shifts, Inner Potential, Absorption, Debye-Waller factors

3. COMPUTATIONAL SCHEME TO CALCULATE INTENSITIES.
e.g. CAVLEED

4. COMPARISON OF EXPERIMENT WITH THEORY: RELIABILITY FACTORS(R FACTORS).

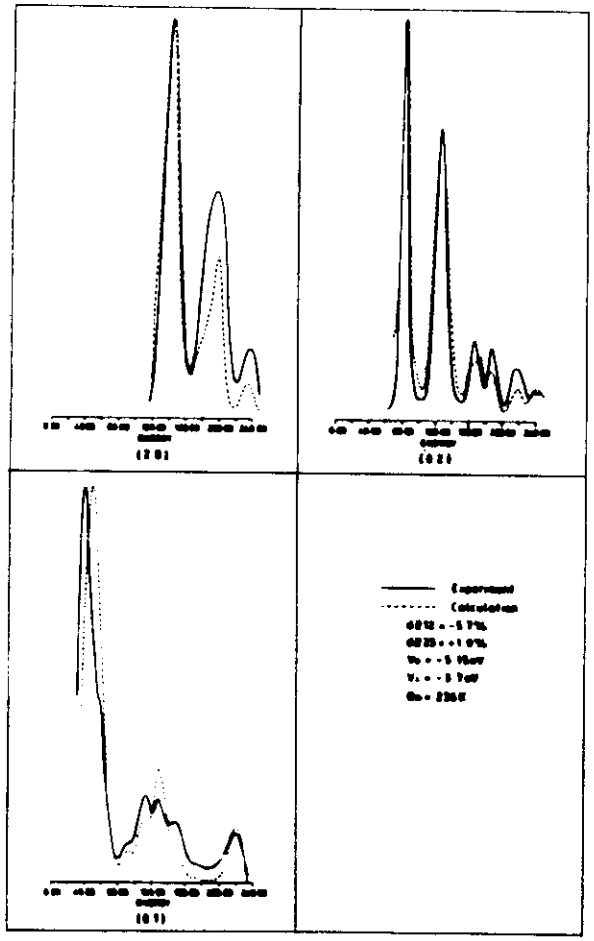

Fig. 1. (a) Best fit theory and experimental $I(V)$ spectra for 7 symmetrically inequivalent beams.

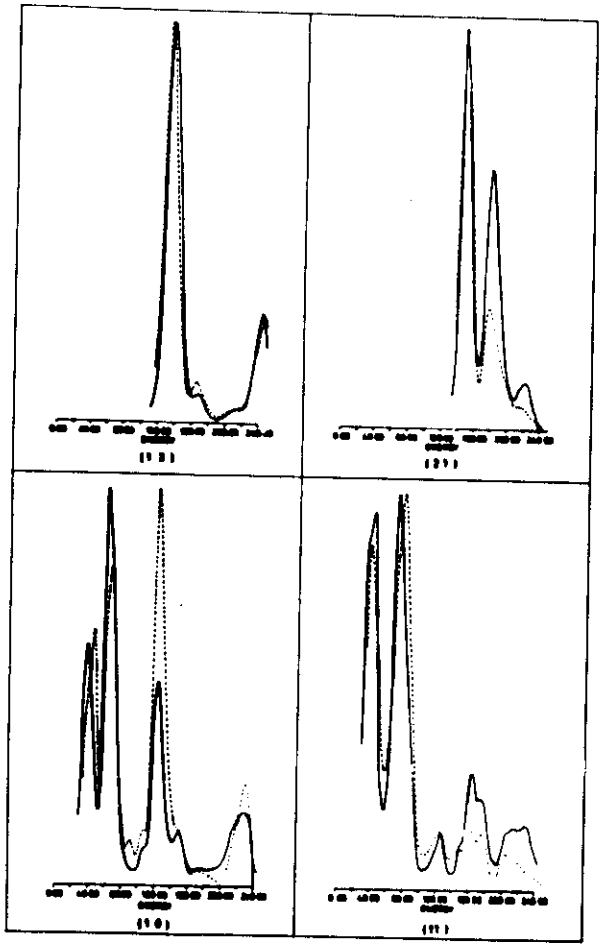

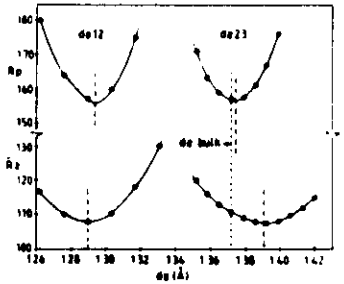

Fig. 1. (b) Pendry (R_p) and Adams (R_2) r-factors as a function of first and second interlayer spacing.

Fig 2

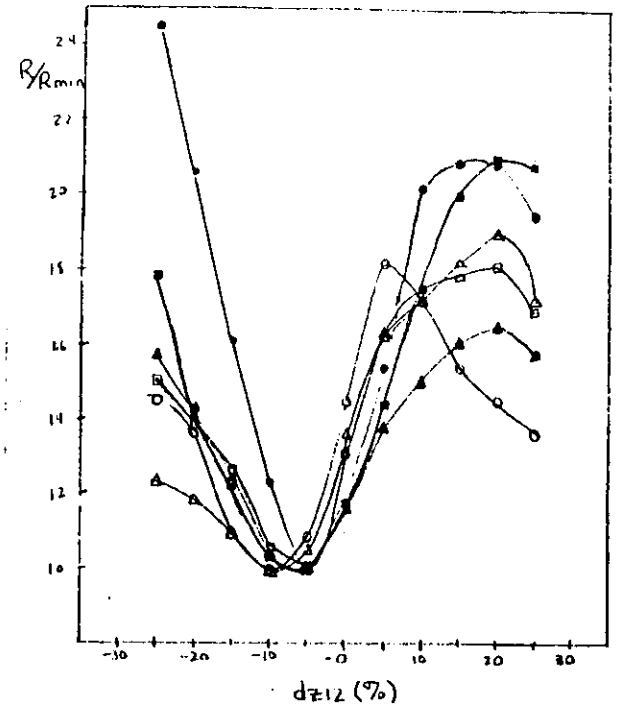

ASSESSMENT OF 6 DIFFERENT R-FACTORS (Pd{110}(1x1))

I. CLEAN METAL SURFACES.

i) TOP LAYER CONTRACTION CF. BULK

INTERLAYER SPACING: 0 – 10%.

E.g. W {100} -7%.

Cu {100} ~0%

i) OSCILLATORY DISPLACEMENTS (STATIC):

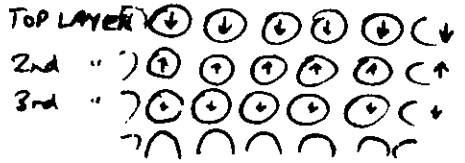

PREDICTED BY LANDMAN

OBSERVED BY ADAMS

e.g. Al.

ii) LATERALLY DISPLACED (1X1):

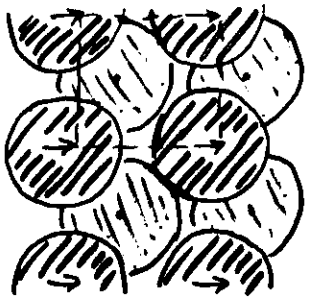

e.g. W(100) (T > 370 K)(?)

Pd (110).

iv) RECONSTRUCTED.

e.g. Pt(110) (1x2)
Au(110) (1x2)

Fcc {110} Reconstruction.

Pt, Au, Ir – CLEAN SURFACE

Cu, Ag, Pd – WITH Cs, Na, etc.

e.g. Pd {110} with Cs:

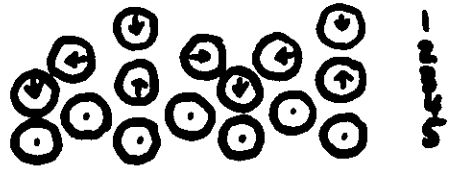

$d_{z_{12}}$ -9%

$d_{z_{23}}$ -1%

$d_{z_{34}}$ +0.5%

Second row pairing:
p = 0.1 Å.

Third row rumpling
δ = 0.1 Å.

Barnes, Lindroos & King, Surf. Sci. 1988.

CO ON METALS FROM LEED:

METAL	STRUCTURE	SITE	d(M-C) Å	d(C-O)
Cu{100}	c(2×2)	1-F	1.90	1.13
Ni{100}	c(2×2)	1-F	1.72	1.13
Pd{100}	c(2√2×√2)R45°	2-F	1.93	1.15
Rh{111}	(√3×√3)R30°	1-F	1.94	1.15
	(2×2)	1-F	1.94	1.15
		2-F	2.03	1.15
Ru{0001}	(√3×√3)R30°	1-F	2.00	1.10

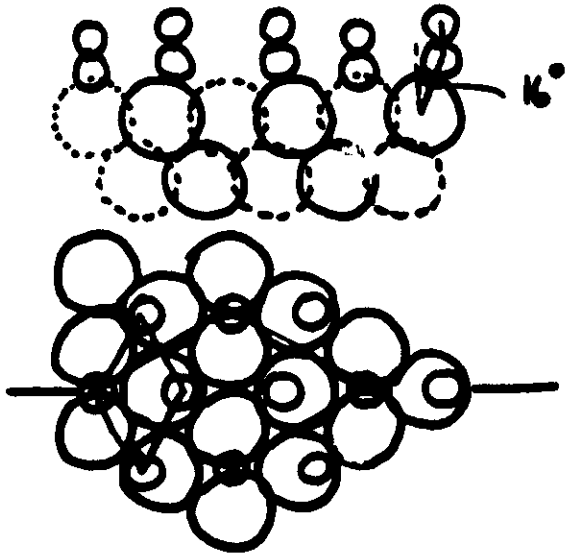

Rh(111)(2×2)-CO

IN LEED, BACK-SCATTERING CROSS SECTION DECREASES WITH DECREASE IN ATOMIC NUMBER.

H A VERY WEAK BACK SCATTERER.

ADVANTAGE: HYDROCARBONS, ONLY NEED TO LOCATE C ATOMS IN STRUCTURE.

DISADVANTAGE: TECHNIQUE ALMOST BLIND TO H ADATOMS.

NOTE: IF SUBSTANTIAL INTENSITY SCATTERED INTO BEAMS PRODUCED BY H ADSORPTION, PROBABLE THAT DISPLACIVE OR RECONSTRUCTIV STRUCTURE FORMED.

E.G. H/Ni{110} AT SATURATION:
(1×2) STRUCTURE, PROBABLY MISSING ROW.

FOR H STRUCTURES: He ATOM DIFFRACTION.

HELIUM ATOM BEAM DIFFRACTION.

(LOW ENERGY ATOM DIFFRACTION, LEAD.)

HELIUM ATOMS AT THERMAL ENERGIES.

e.g. 300 K, $\lambda = 0.57$ Å.

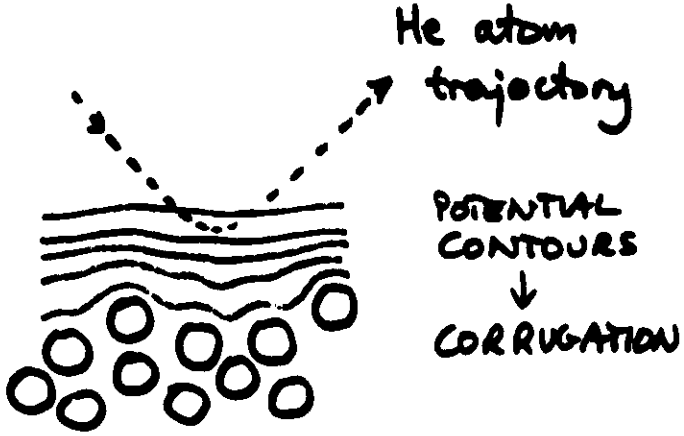

He diffraction : H/Ni {110}.

LEED : low coverage, weak (2×1)
saturation, strong (1×2).

He diff :

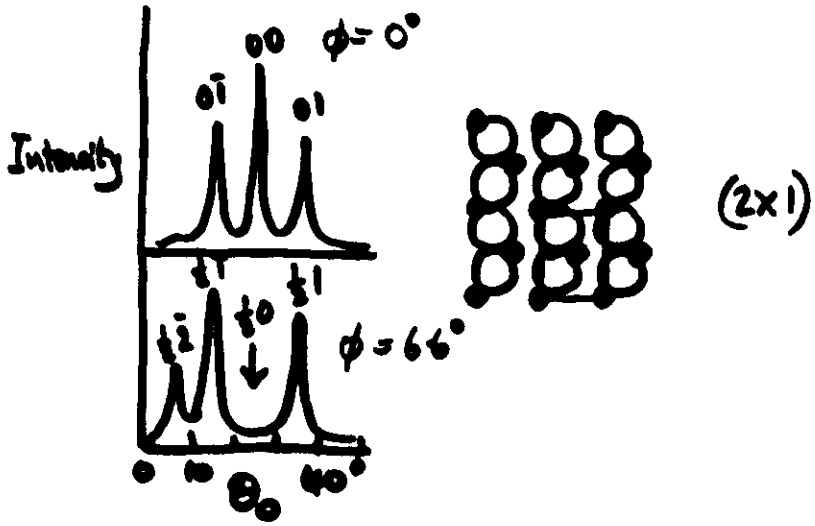

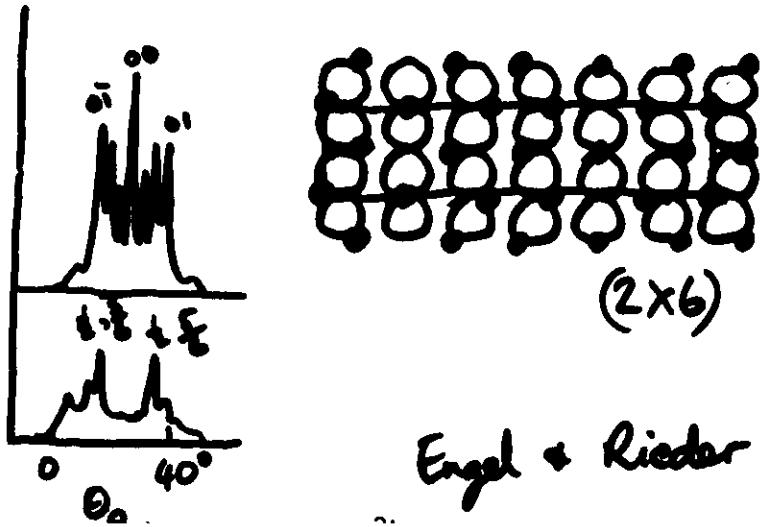

Engel + Rieder

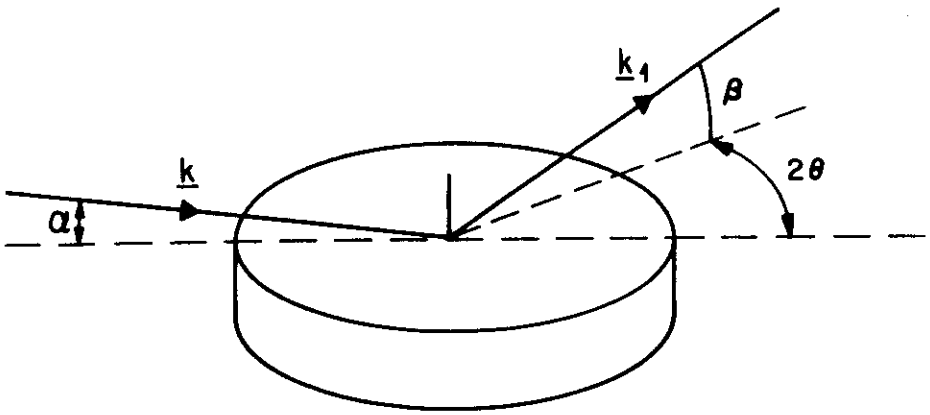

2D X-ray Diffraction.

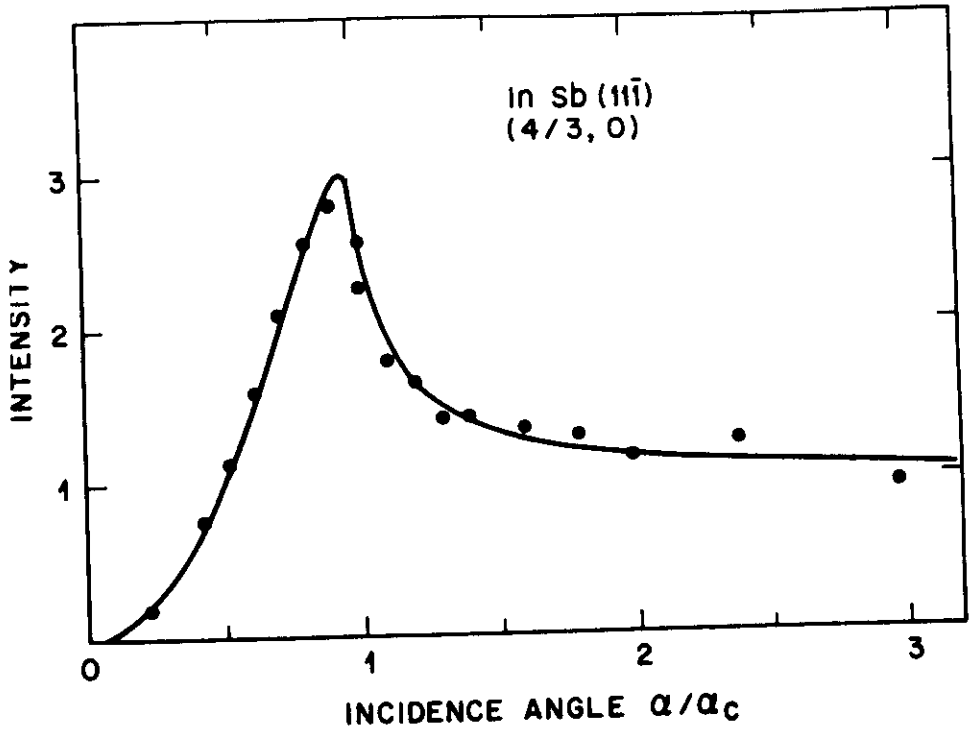

TOTAL EXTERNAL REFLECTION:

Refractive index n : $\cos \alpha_c = n$

Typically $\alpha_c = 0.3°$ (5 mrad)

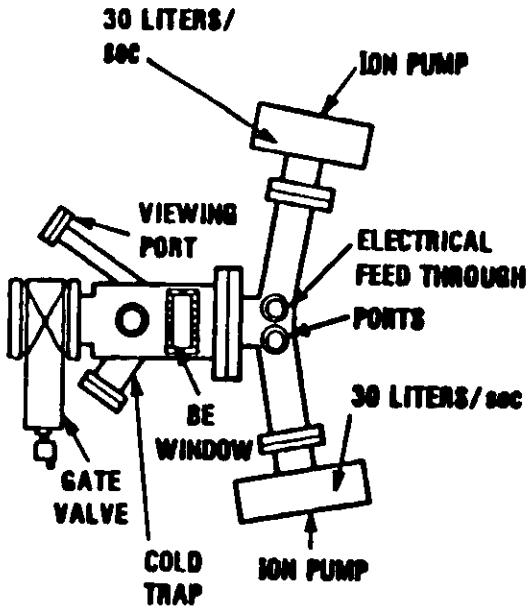

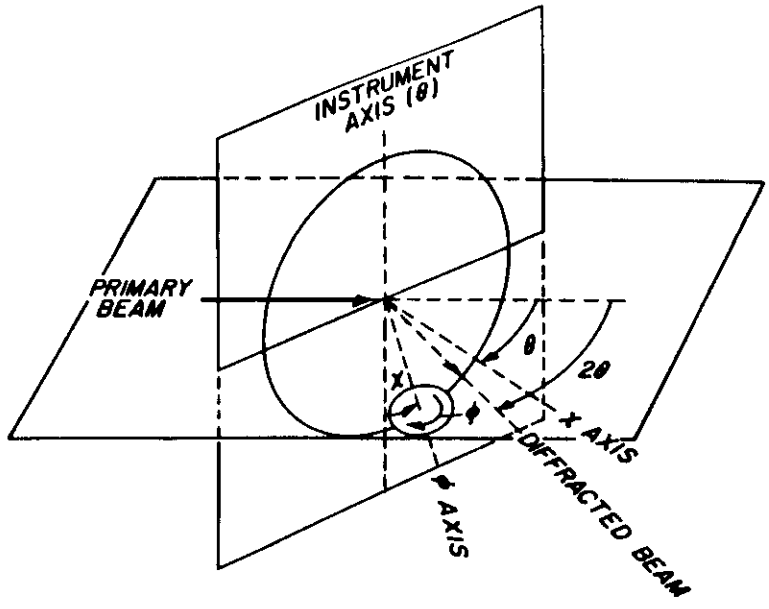

X-RAY TRANSFER CELL

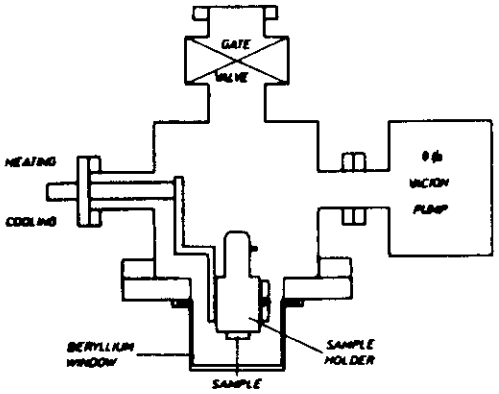

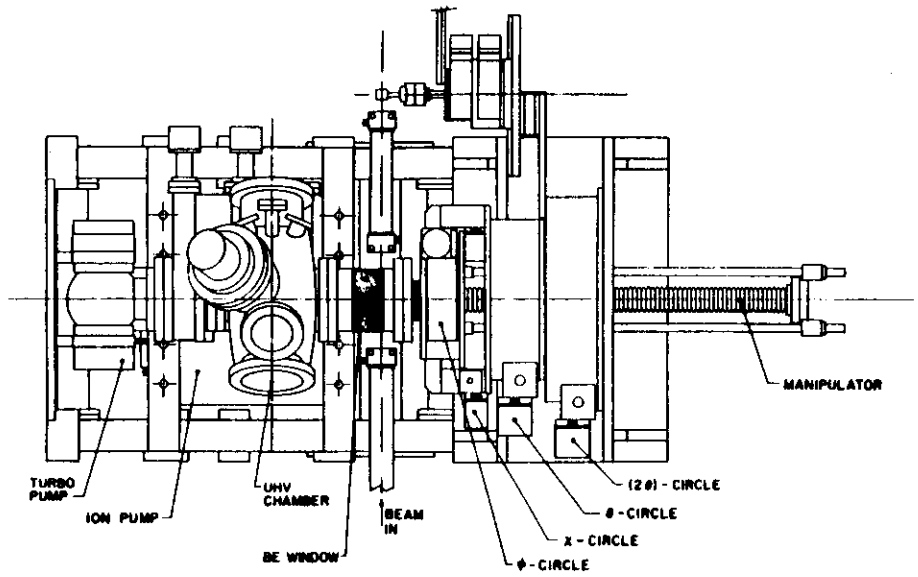

STRUCTURES: Ge {100} (2x1);
Pb/Cu {110}; Au {110} (1x2);
In Sb {111} (3x3); O/Cu {110} (2x1)
In Sb {111} (2x2); Si {111} (7x7)
W {100} ; Pb/Ge {111}

Fuoss, Liang, Eisenberger,
in 'Synchrotron Radiation Research:
Advances in Surface & Low Dimensional
Science', ed. BACHRACH, PLENUM, 1986.

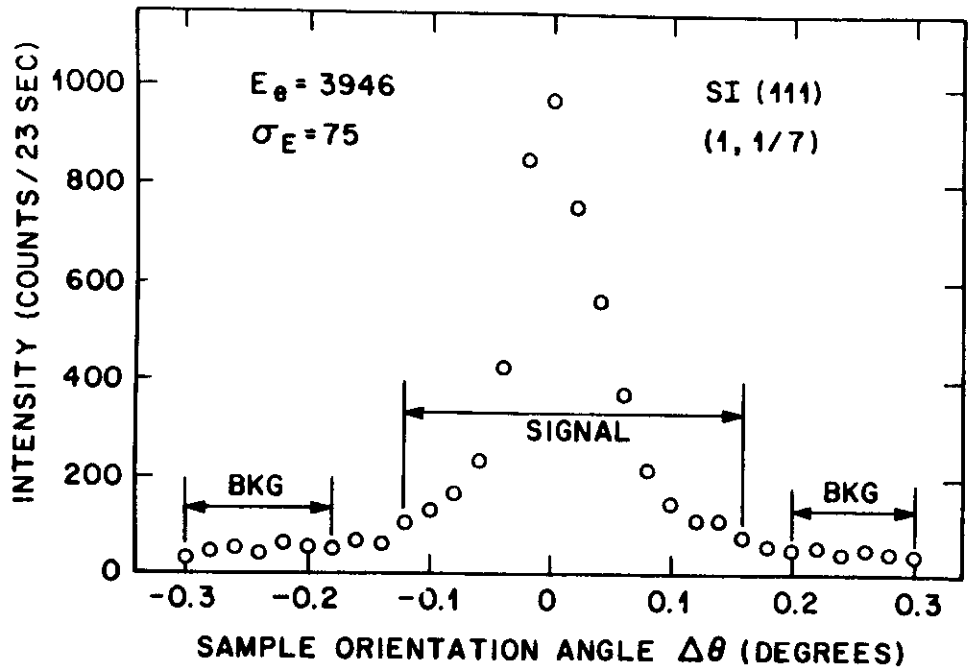

THE STORY SO FAR.....

1. CLASSIFICATION OF STRUCTURES

2. STRUCTURAL TOOLS.

   a. LONG RANGE ORDER:

      1. LEED
         PATTERNS – SYMMETRY.
         I-V SPECTRA – COMPLETE STRUCTURE
         MULTIPLE SCATTERING DOMINATES.

      2. HELIUM BEAM DIFFRACTION
         HYDROGEN ADSORPTION.

      3. 2D X-RAY DIFFRACTION
         ATTRACTION: SINGLE SCATTERING DOMINATES
         PROBLEM - EXPERIMENTALLY VERY DEMANDING.

2. STRUCTURAL TOOLS (CONT.)

   b. LOCAL STRUCTURE, DIFFRACTION

      1. PHOTOELECTRON DIFFRACTION

      2. SEXAFS

   c. REAL SPACE TECHNIQUES.

      1. INCIDENT ION BEAMS

      2. MICROSCOPIES

   d. INDIRECT TECHNIQUES

      1. VIBRATIONAL SPECTROSCOPIES

      2. NEXAFS

      3. ARUPS

      4. THERMAL DESORPTION

LOCAL ELECTRON SCATTERING METHODS.

SOURCE OF ELECTRONS WITHIN THE CRYSTAL, PRODUCED (E.G.) BY PHOTOEMISSION:

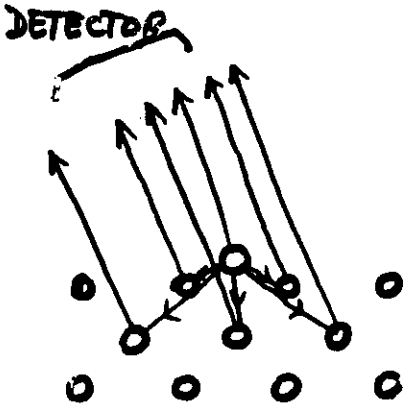

PHOTOELECTRON DIFFRACTION

INTERFERENCE → INTENSITY VARIATIONS AS:

(i) ANGLE OF COLLECTION

(ii) PHOTOELECTRON ENERGY

ARE VARIED.

CORE LEVEL PHOTOEMISSION.

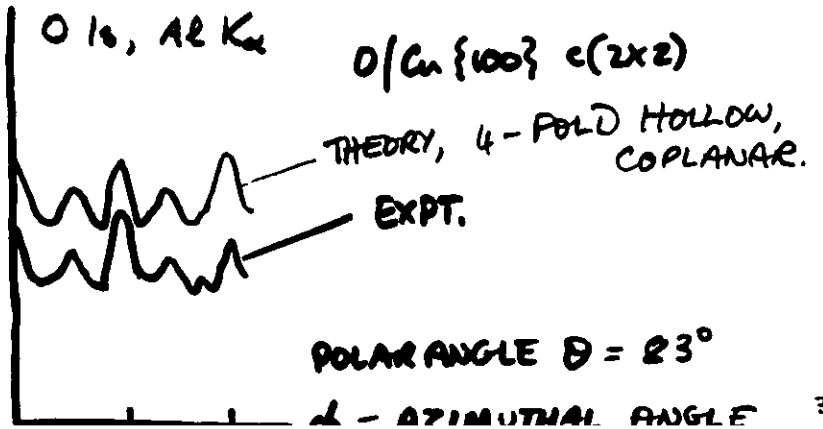

SEXAFS

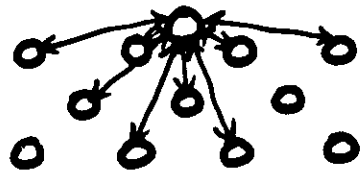

BACKSCATTERED WAVES INTERFERE WITH OUTGOING EMITTED WAVE → MODULATION IN PHOTOIONISATION CROSS SECTIONS - (X-RAY ABSORPTION) - AS PHOTON ENERGY IS VARIED.

NEAREST SHELL BOND LENGTH ACCURACY: ± 0.02 Å.

UP TO 4 SHELLS CAN BE DETECTED.

NEEDS SYNCHROTRON RADIATION.

SURFACE EXAFS

Raw data from half monolayer

SULPHUR on NICKEL {110}

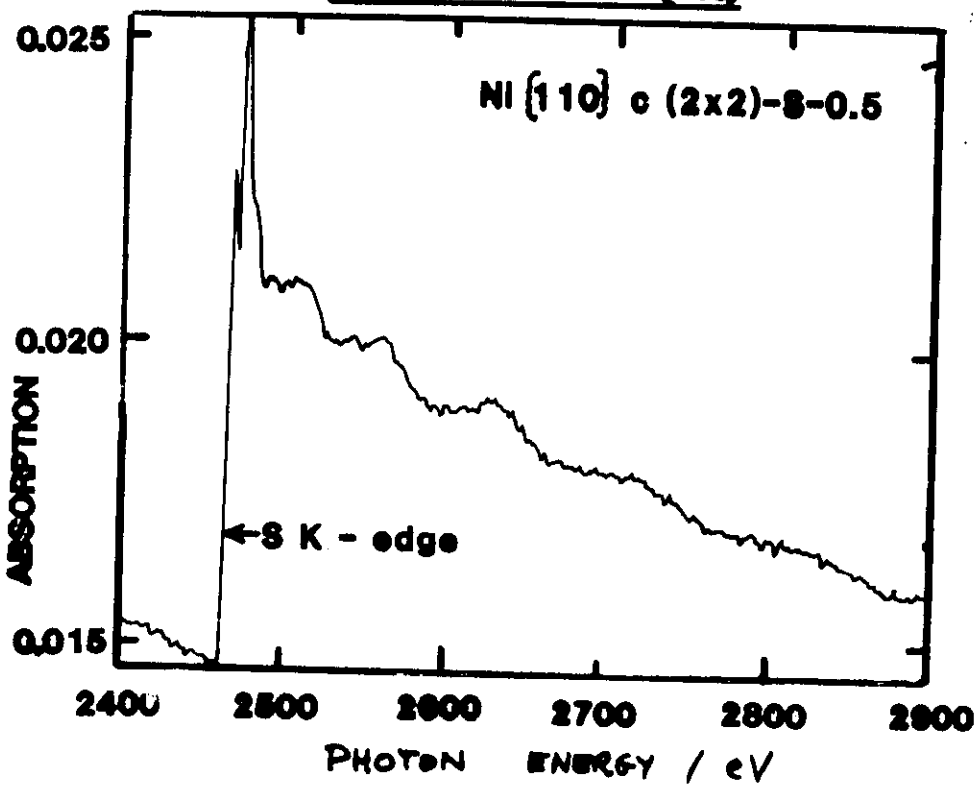

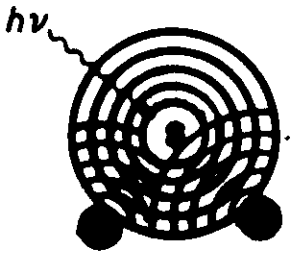

ISS : N on W{100}

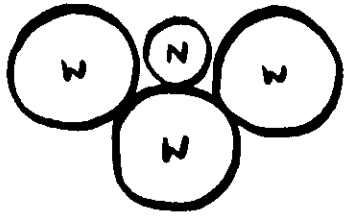

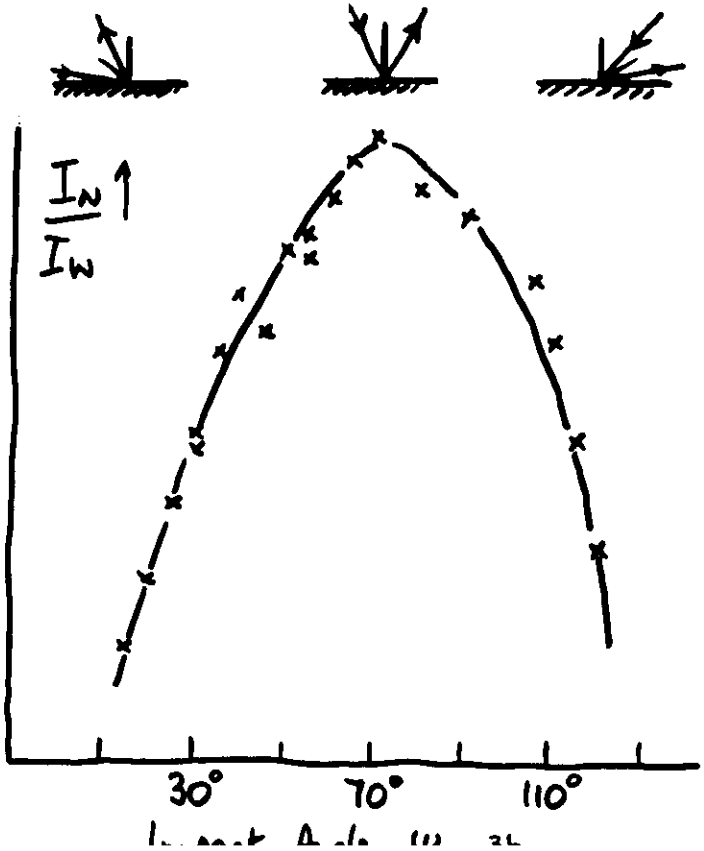

ION SCATTERING SPECTROSCOPY:

β-N and β_3-CO on W{100}.

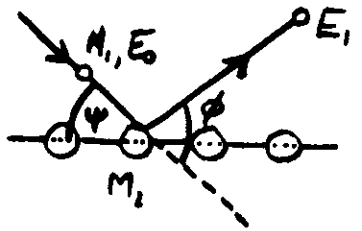

He^+ incident ions, $E_0 = 1000$ eV.

$$\frac{E_1}{E_0} = \left\{ \frac{1}{1 + M_2/M_1} \left[\cos\phi \pm \left\{ (M_2/M_1)^2 - \sin^2\phi \right\}^{1/2} \right] \right\}^2$$

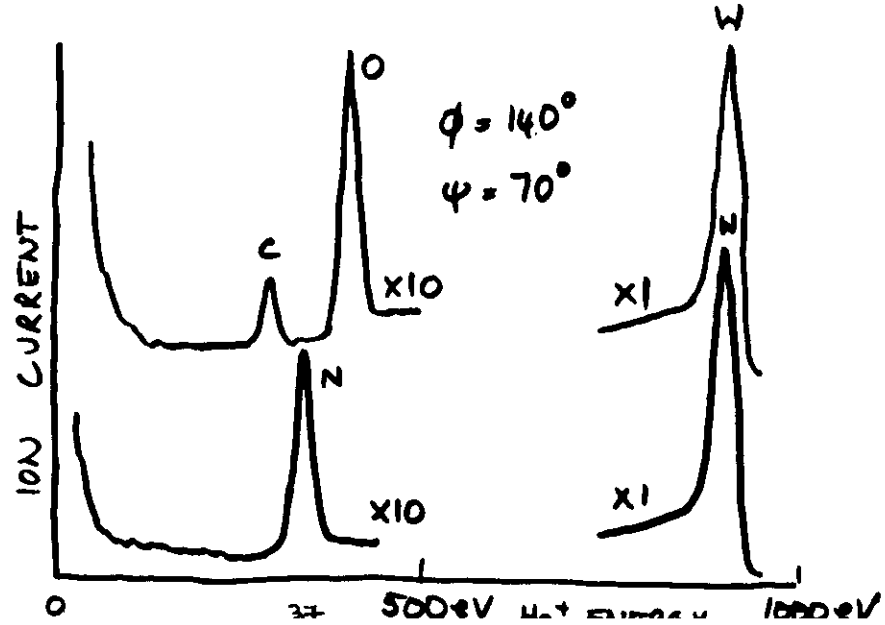

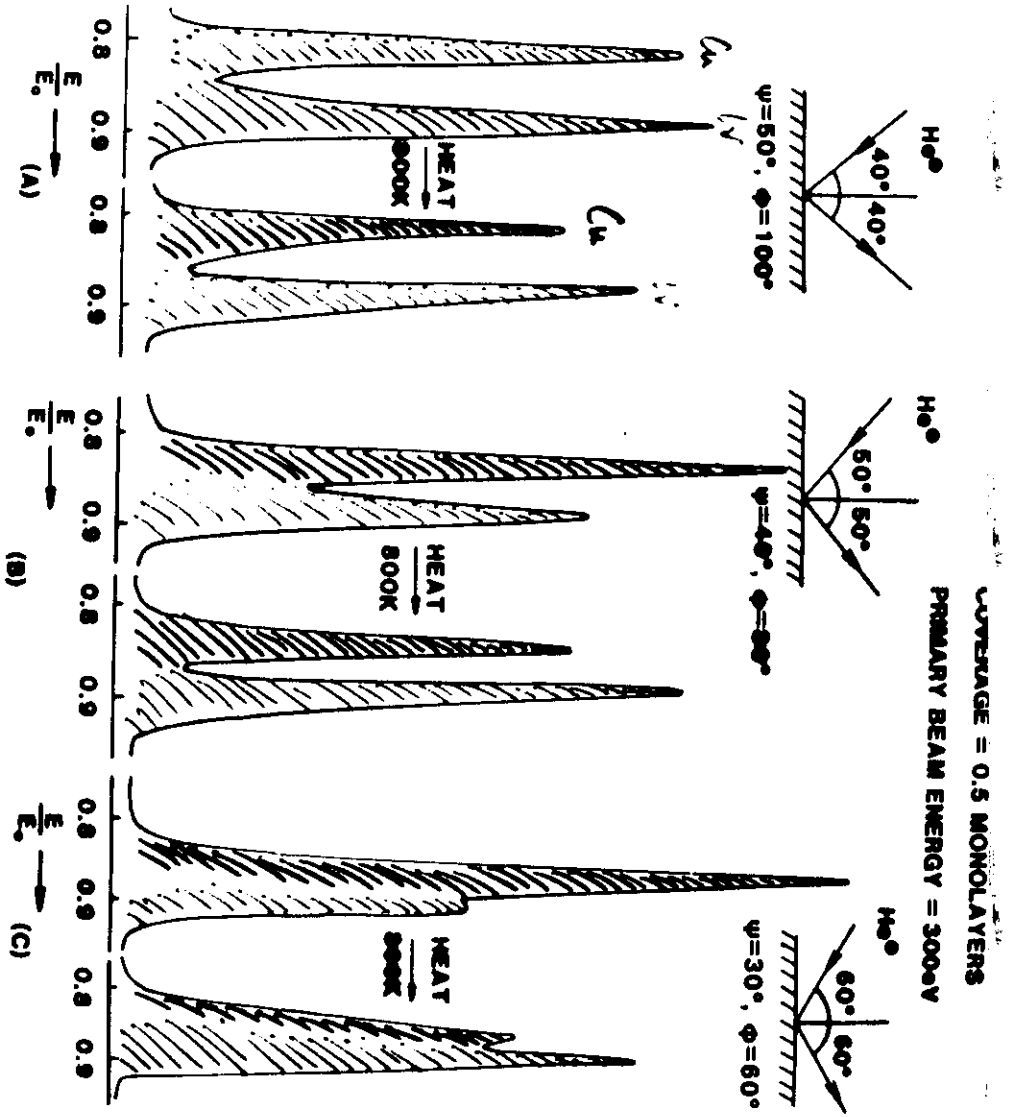

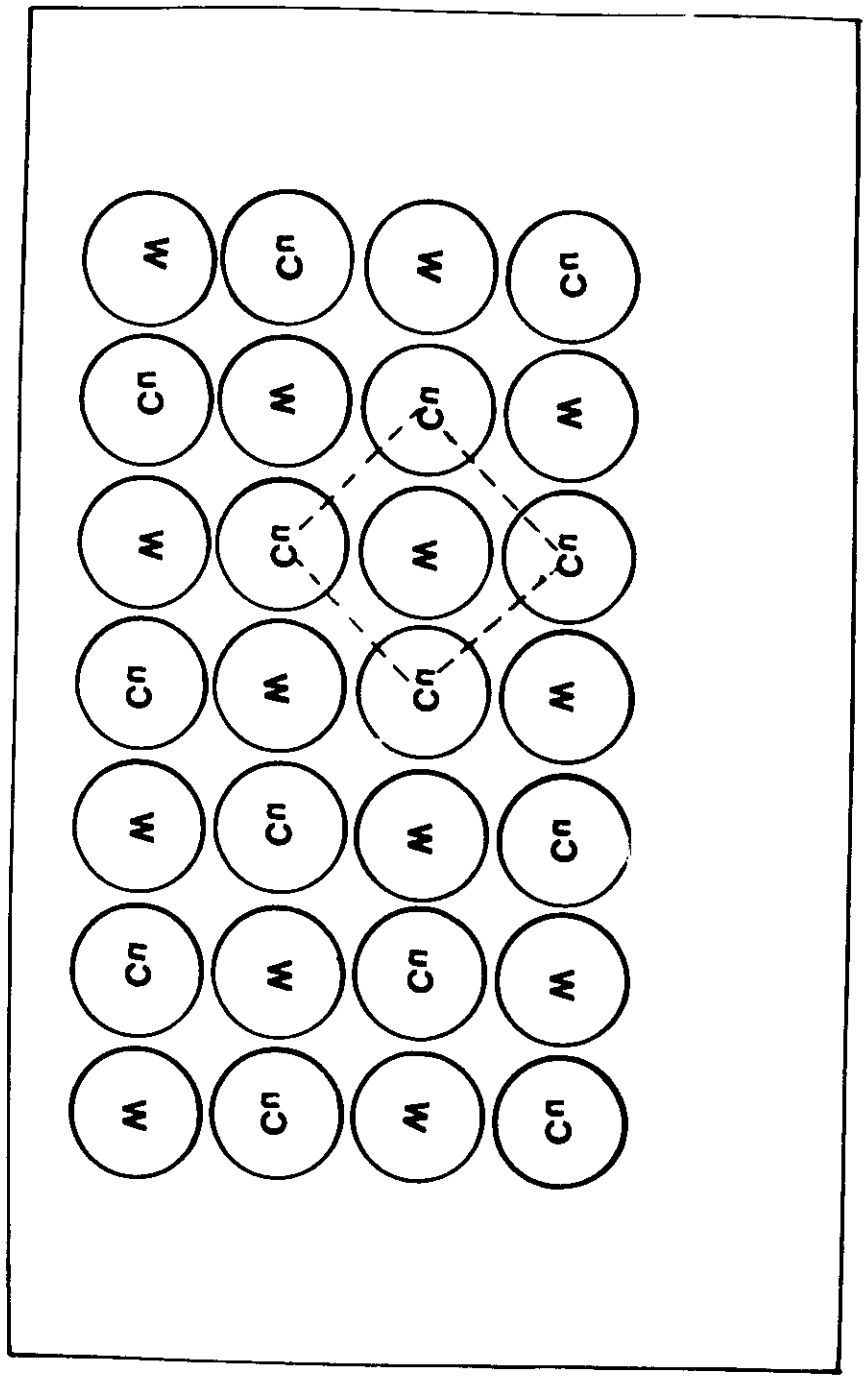

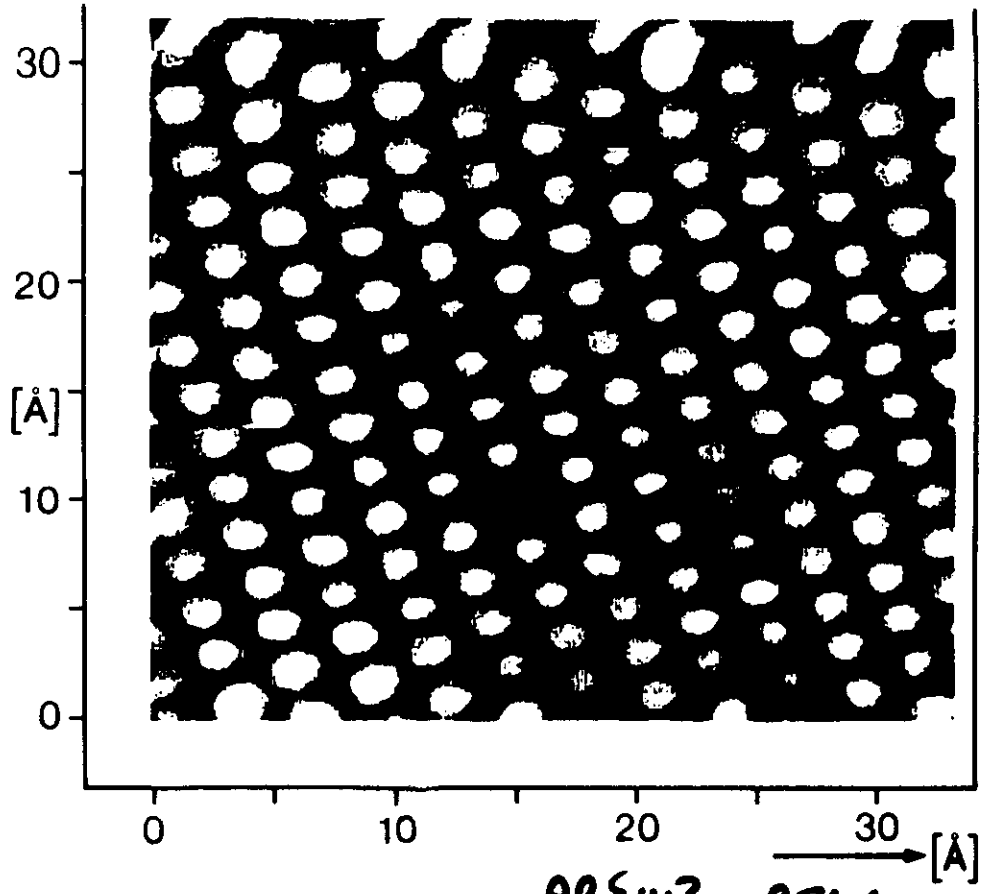

AR{111}: BEHM

SCANNING TUNNELING MICROSCOPY

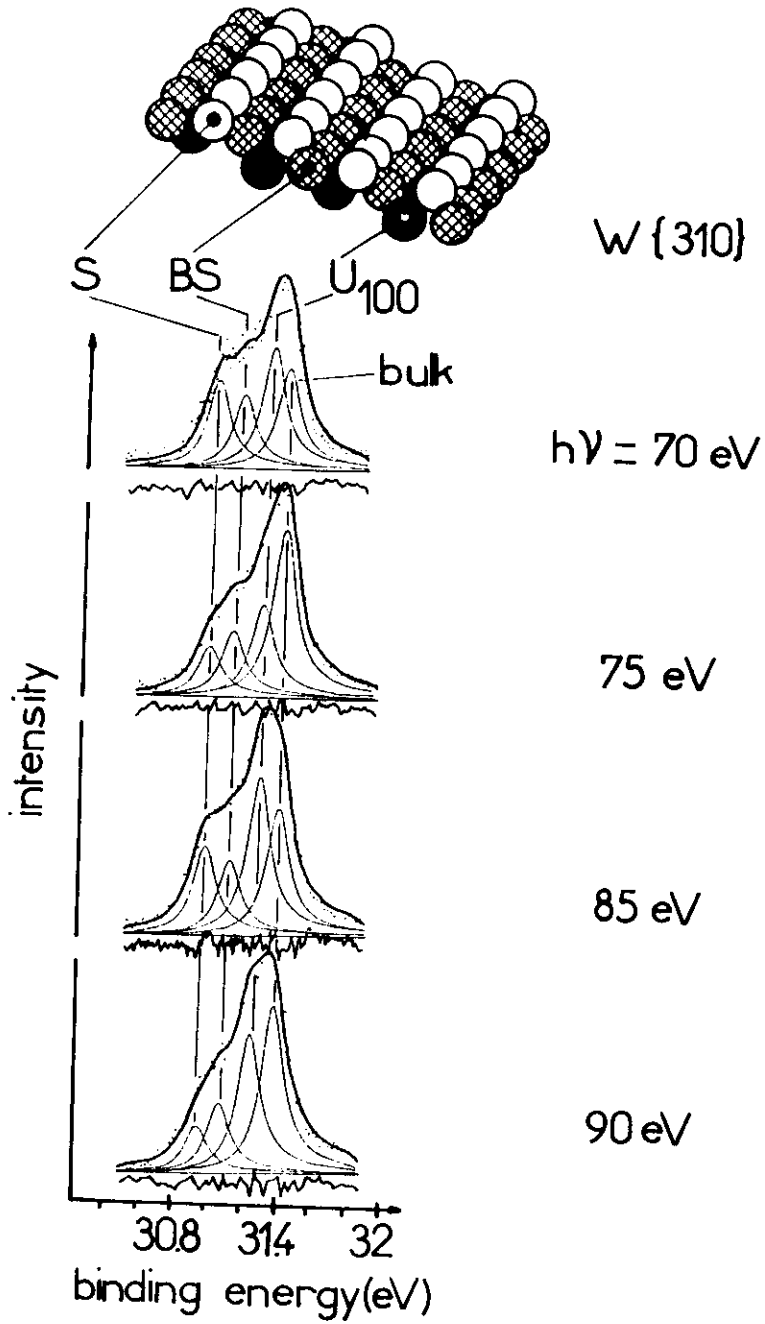
S
BS
U100
bulk
W {310}
hν = 70 eV
75 eV
85 eV
90 eV
intensity
30.8
31.4
32
binding energy(eV)

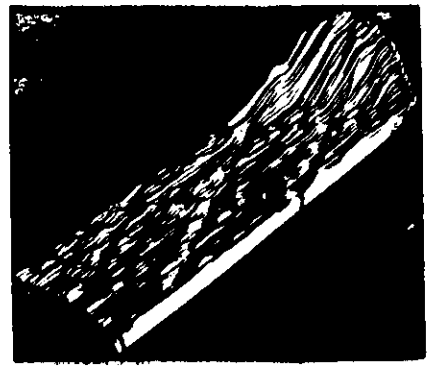

REAL SPACE TECHNIQUES.

2. INCIDENT ION TECHNIQUES.

LOW ENERGY : 300 eV to 2000 eV ions.

BINARY COLLISION : SURFACE ANALYSIS + SHADOWING.

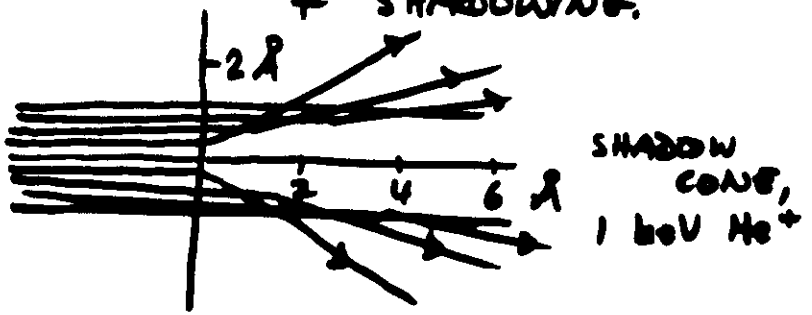

HIGH ENERGY, ~1 MeV, SHADOW CONE NARROW. → TOP LAYER SPACINGS.

II. MICROSCOPIES.

QL. MICR.

FIELD ION MICROSCOPE

STM

INDIRECT TECHNIQUES.

VIBRATIONAL SPECTROSCOPY

RAIRS HREELS

NEXAFS.

ARUPS.

THERMAL DESORPTION.

COVERAGE-DEPENDENT FREQUENCY SHIFTS FROM ADSORBATES.

1.) Change in binding site

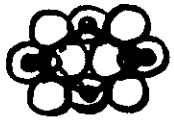

e.g. CO on Pt {111}

- ω_{C-O} (linear) = 2065 cm^{-1}
- ω_{C-O} (bridged) = 1871 cm^{-1}

2.) Change in chemisorption complex geometry

e.g. H on W{100}

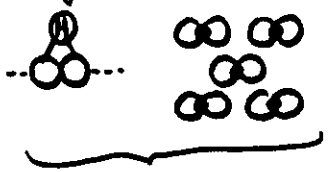

$\theta \leq 0.12$

ω_s = 1250 cm^{-1}

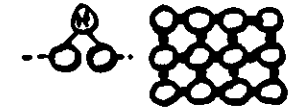

θ = 1.0

ω_s = 1040 cm^{-1}

3.) Neither 1.) nor 2.) : dipole coupling and subtle bonding shifts.

Continuous shift in ω as coverage is increased.

e.g. CO on Pt single crystals : $\Delta\omega \simeq 35\ cm^{-1}$
CO on Pd{100} : $\Delta\omega \simeq 100\ cm^{-1}$
CO on Ag : $\Delta\omega = -30\ cm^{-1}$

FREQUENCY SHIFTS INDUCED BY DIPOLE COUPLING

Isolated species (singleton) $\omega_{C-O} = \omega_o$

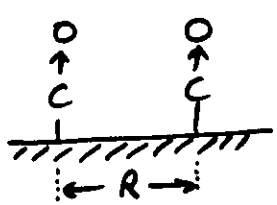

In-phase mode

$\omega_o + \Delta\omega$

Dipole active

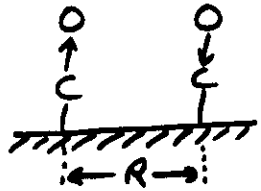

Out-of-phase mode

$\omega_o - \Delta\omega$

Dipole inactive

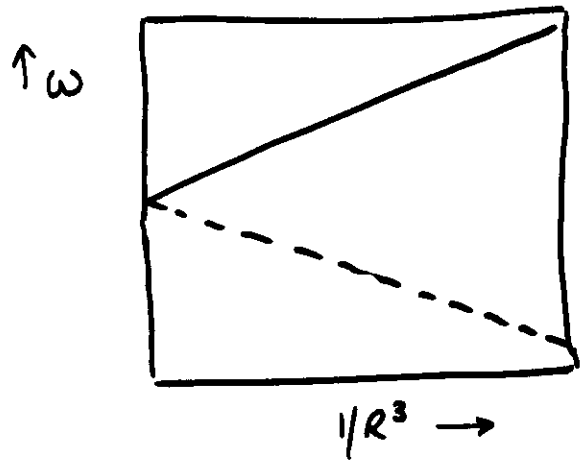

RAIRS : } only — observed.
Spec. HREELS: }

Off-spec. HREELS (impact scattering) : — and ---

Angle-resolved photoemission:

Bonding of CO to Pt{110}:

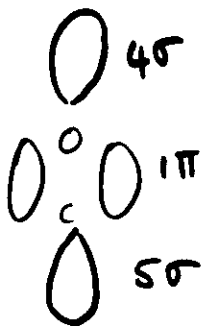

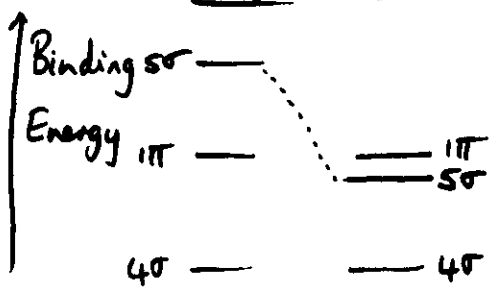

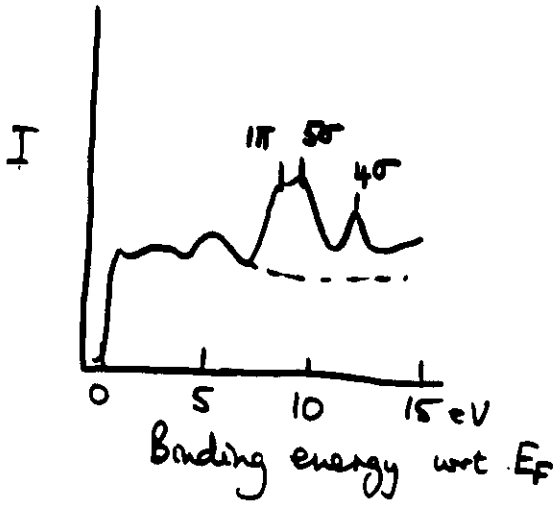

CO on Pt{100}.

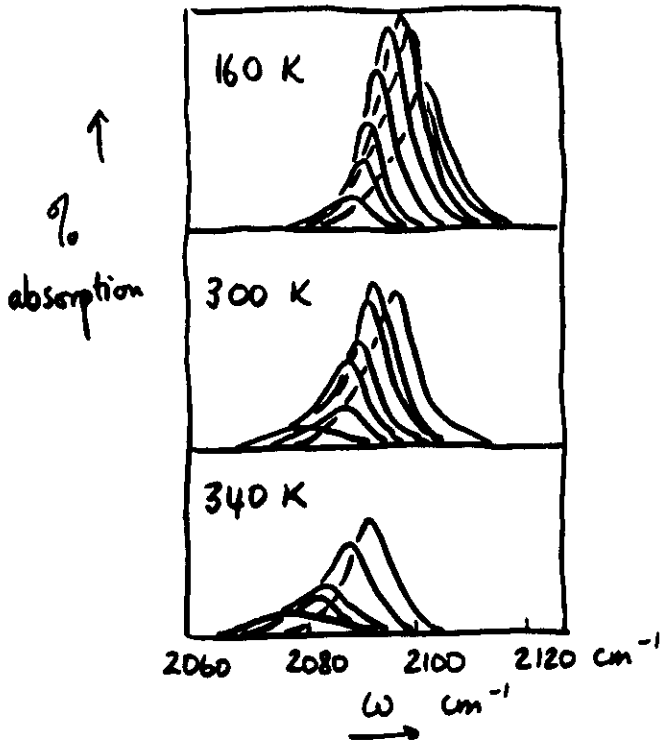

Dilution limit from isotopic mixtures,
$^{12}CO/^{13}CO$: $\omega_s = 2062\ cm^{-1}$

CONCLUSION:

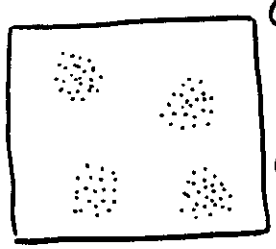

① Islands of condensed phase formed even at lowest coverage.

② At fixed Θ, island size depends on crystal temperature.

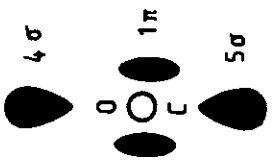
4σ
1π
5σ
O
C

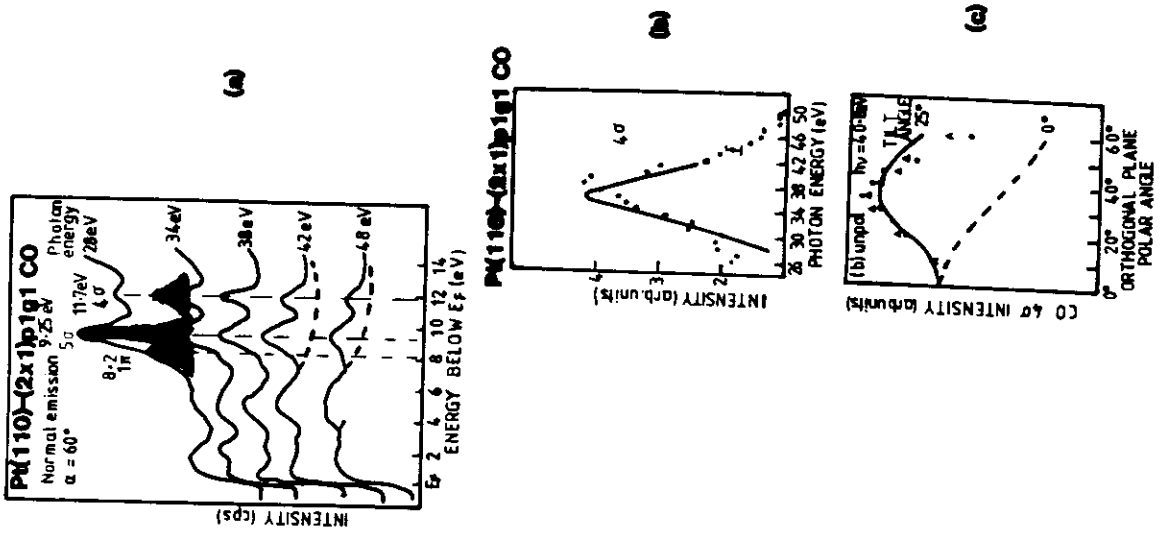
(a)
(b)
(c)
Pt(110)-(2x1)p1g1 CO
Normal emission
α = 60°
Photon energy
9.25eV
11.7eV
28eV
34eV
38eV
42eV
48eV
4σ
5σ
1π
INTENSITY (cps)
ENERGY BELOW EF (eV)
PHOTON ENERGY (eV)
INTENSITY (arb.units)
ORTHOGONAL PLANE
POLAR ANGLE

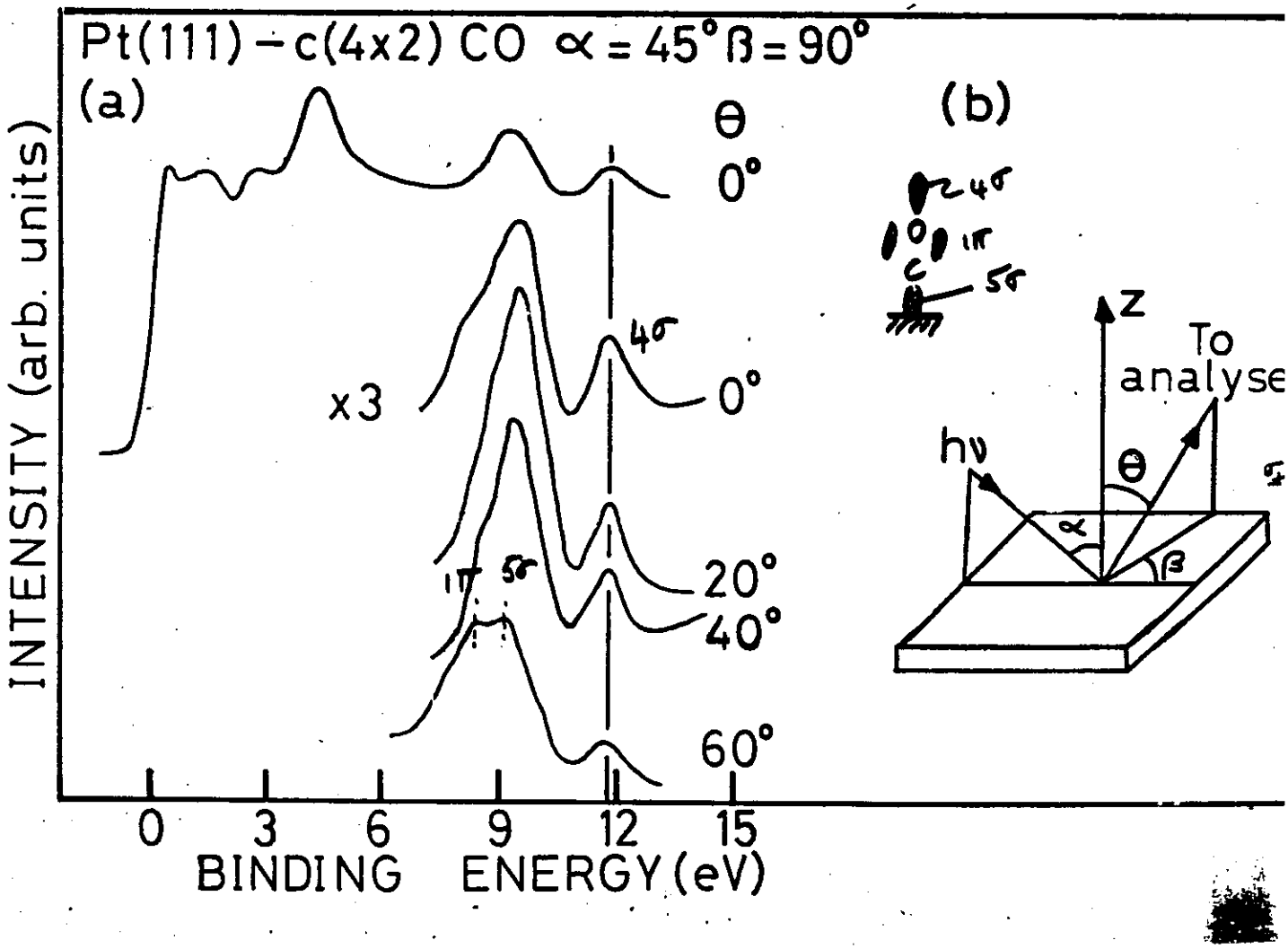
Pt(111) – c(4x2) CO α = 45° β = 90°
(a)
(b)
θ
0°
0°
20°
40°
60°
x3
4σ
1π
5σ
INTENSITY (arb. units)
0
3
6
9
12
15
BINDING ENERGY (eV)
hν
z
To analyse
α
β

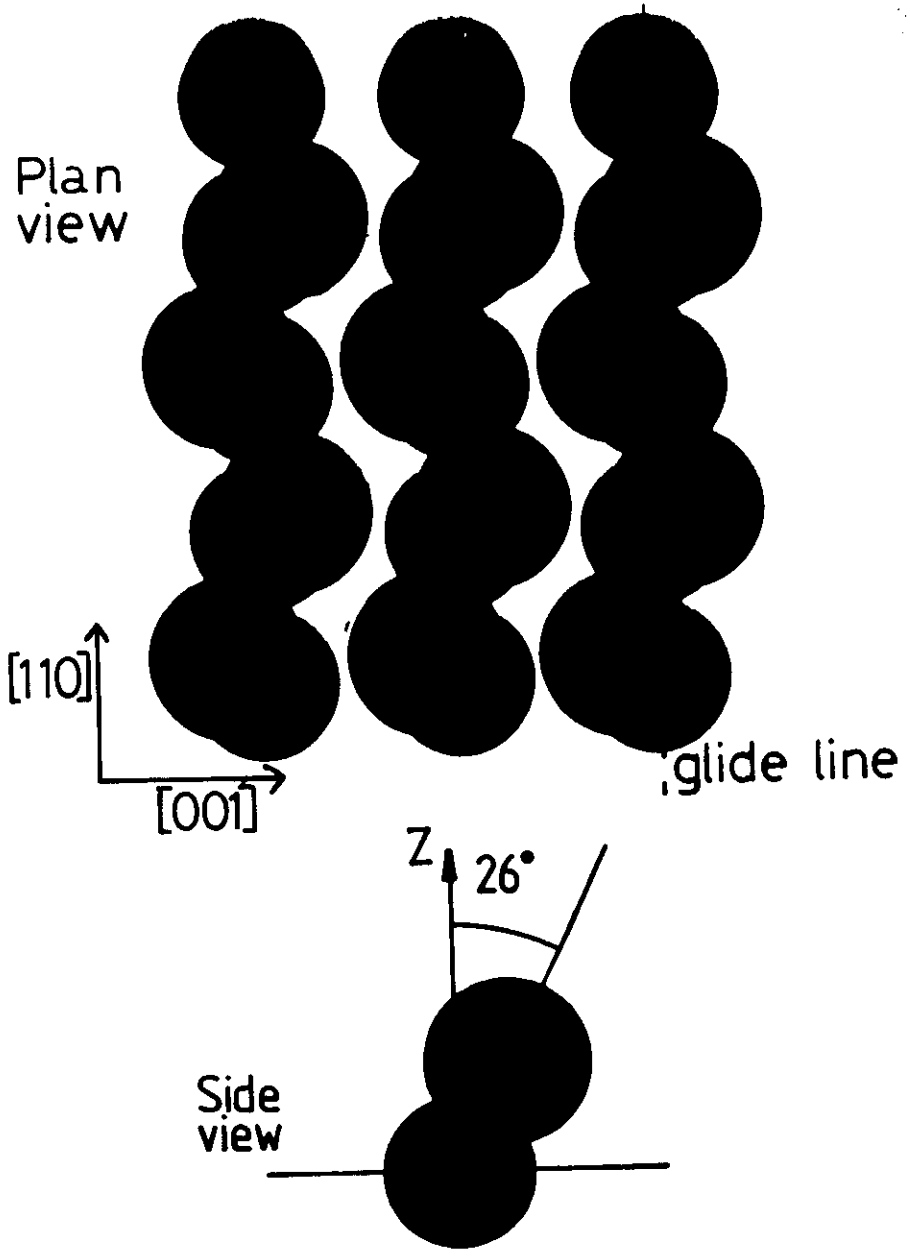
Plan
view
[110]
[001]
glide line
Z
26°
Side
view

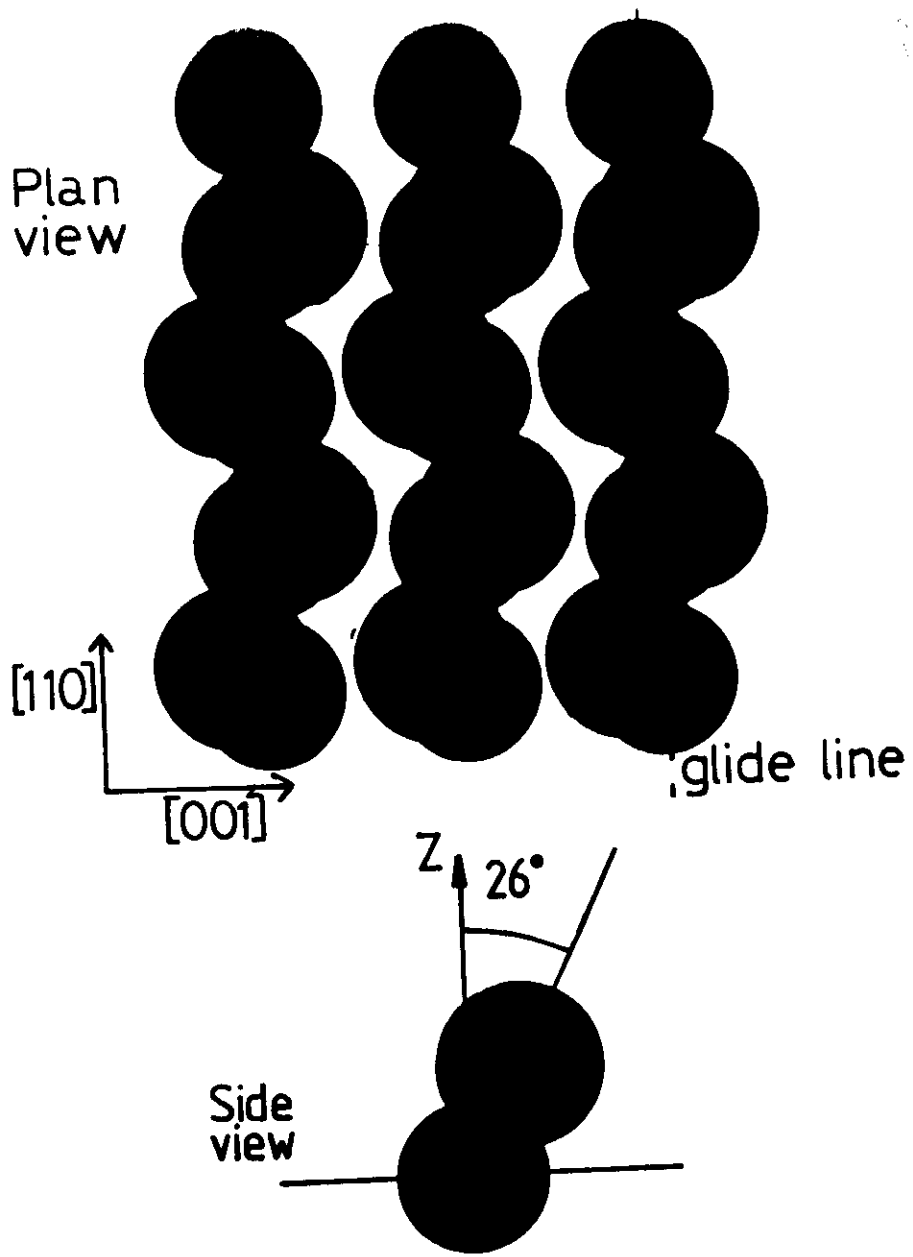
Plan
view
[110]
[001]
glide line
Z
26°
Side
view

Angle-resolved photoemission.

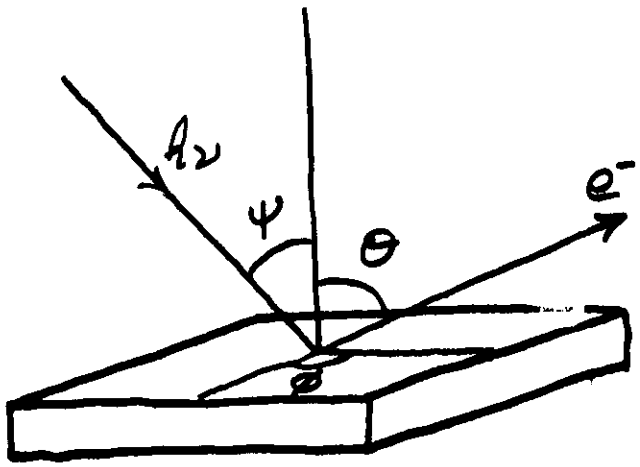

$$E_{kin} = h\nu - \phi - E_{b.e.} \qquad (1)$$

$$E_{kin}^{1/2} \sin\theta = k_{\parallel}$$

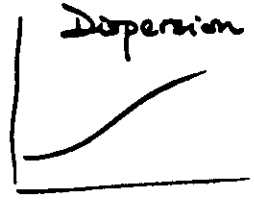

ORIGINS OF MULTIPLE PEAKS IN DESORPTION SPECTRA.

(1) CRYSTALLOGRAPHY

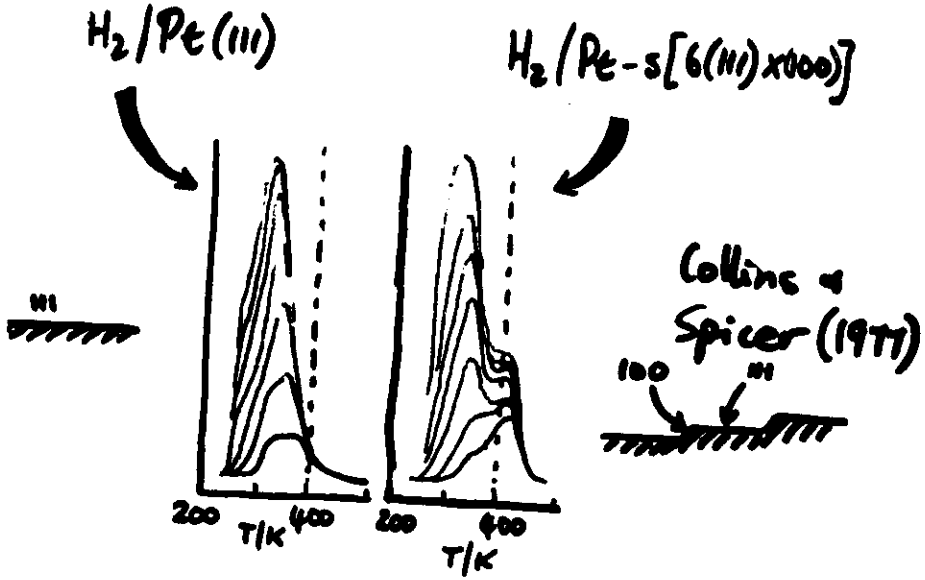

(2) SITE CONFIGURATION

CO/Pt(111) Bonzel & Ku (1973)

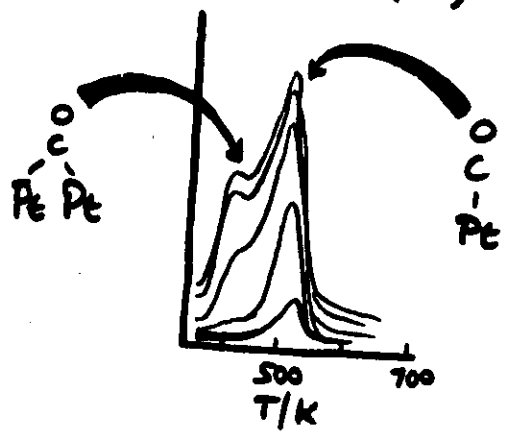

③ Molecular Integrity

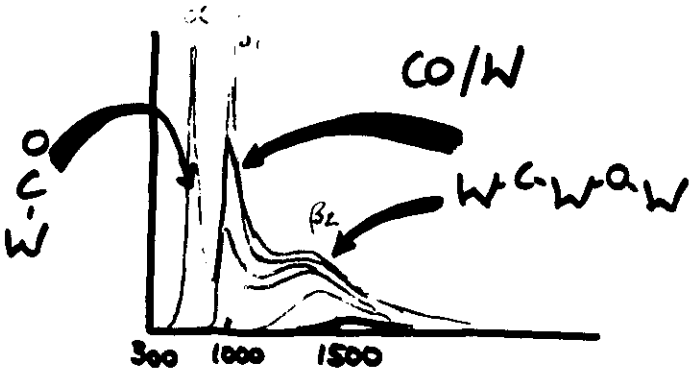

④ Lateral Interactions

β_1, β_2 states on W(110)

$\omega = 20$ kJ mol^{-1}

Guyemer + King 1978

⑤ Desorption - Reconstruction.

CO / Pt {110}

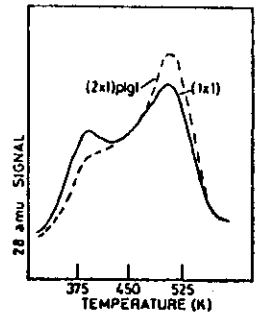

Fig. 13. The CO desorption spectra from the (2 × 1)plgl phase (dashed line) and saturated (1 × 1) phase (full line) superimposed on top of each other.

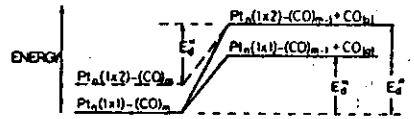

Fig. 12. A schematic illustration of the energy levels associated with the desorption of CO from Pt{110}, leaving either a (1 × 1) or (1 × 2) substrate.

Bare, Hofmann and King. 1984.

Split peak in desorption spectra due to formation of (1x2) surface from (1x1) surface as coverage is reduced.

NEXAFS AT GRAZING INCIDENCE:

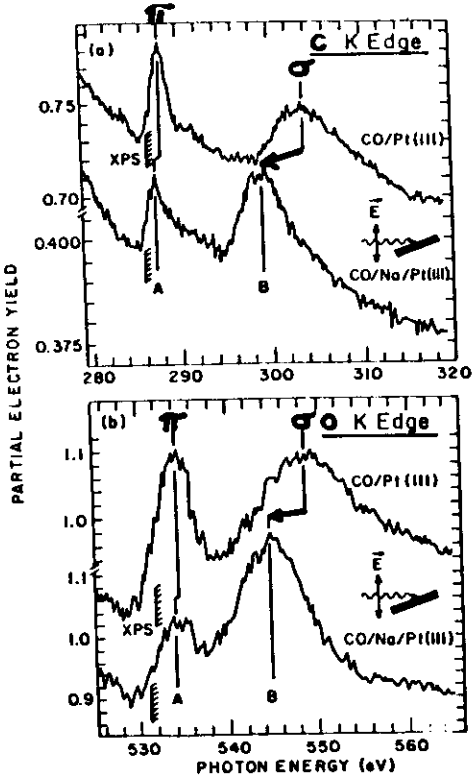

Na INDUCES A 4eV SHIFT OF σ RESONANCE

⇒ STRETCH OF C-O BOND

USE EMPIRICAL RULES FOR VARIATION OF BOND LENGTH WITH RESONANCE POSITION

$$\Delta R = 0.12 \pm 0.03\ \text{Å}$$

III

THE MISSING VARIABLE:

BOND LENGTH.

DIFFICULT TO MEASURE WITH SUFFICIENT ACCURACY.

LEED:

- ACCURATE TO ± 0.05 Å
- ONLY FEASIBLE FOR RELATIVELY SIMPLE, WELL-ORDERED STRUCTURES
- DYNAMICAL ANALYSIS

SEXAFS:

- POTENTIAL FOR ± 0.01 Å RELIABILITY
- DOES NOT DEPEND ON LONG RANGE ORDER.
- KINEMATIC ANALYSIS

EXAFS (Extended X-Ray Absorption Fine Structure)

Absorption fine Structure, after background subtraction: $\chi(k)$

$$\chi(k) = \sum_i A \sin(2kR_i + \phi_i)$$

R_i: interatomic spacing

ϕ_i: phase shift $= 2\phi_a + \phi_b$

SEXAFS (Surface EXAFS)

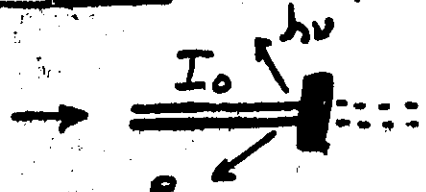

SURFACE SENSITIVITY ACHIEVED BY: (i) AUGER YIELD MEASUREMENT

(ii) SECONDARY ELECTRON YIELD

(iii) PHOTODESORPTION

(iv) FLUORESCENCE YIELD

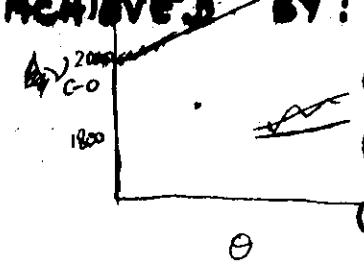

EXTENDED X-RAY ABSORPTION FINE STRUCTURE

Co-author: Geraldine LAMBLE

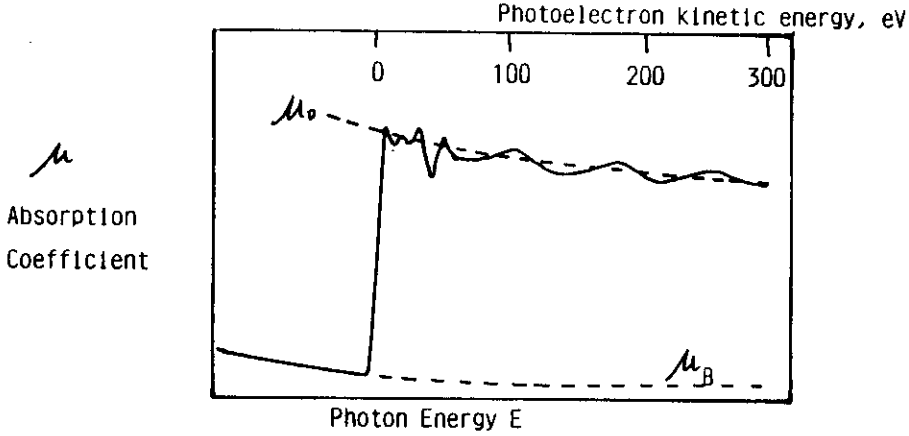

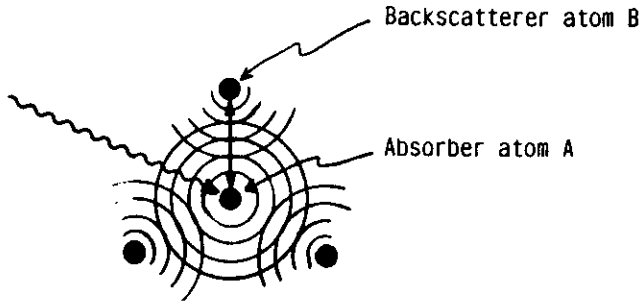

Modulation of $\chi(k) = \dfrac{(\mu - \mu_0)}{(\mu_0 - \mu_B)}$

depends on: scattering amplitude from B, F(k)

and: phase shift function $\phi(k)$

and: the A - B spacing R_1.

The EXAFS expression for the absorption $\chi(k)$:

$$\chi(k) = \sum_i \{N_i |F_i(k)| \times \exp(R_i/\lambda(k)) \times \exp(-2k^2\sigma_i^2) \times \sin(2kR_i + \phi_i)/kR_i^2$$

N_i = no. of nearest neighbours in a shell at distance R_i from absorber atom.

$\phi_i = 2\phi_a(k) + \phi_{b_i}(k)$

↑ phase shift due to absorber atom

↖ phase shift due to backscattering atoms in shell i.

ANHARMONICITY CORRECTION:

$$\chi(k) = \sum_i N_i |F_i(k)| \{S_i^2(k) + A_i^4(k)\}^{1/2} \times \sin(2kR_i + \phi_i(k) + \Sigma_i(k)/kR_i^2$$

DARESBURY LABORATORY SYNCHROTRON RADIATION SOURCE

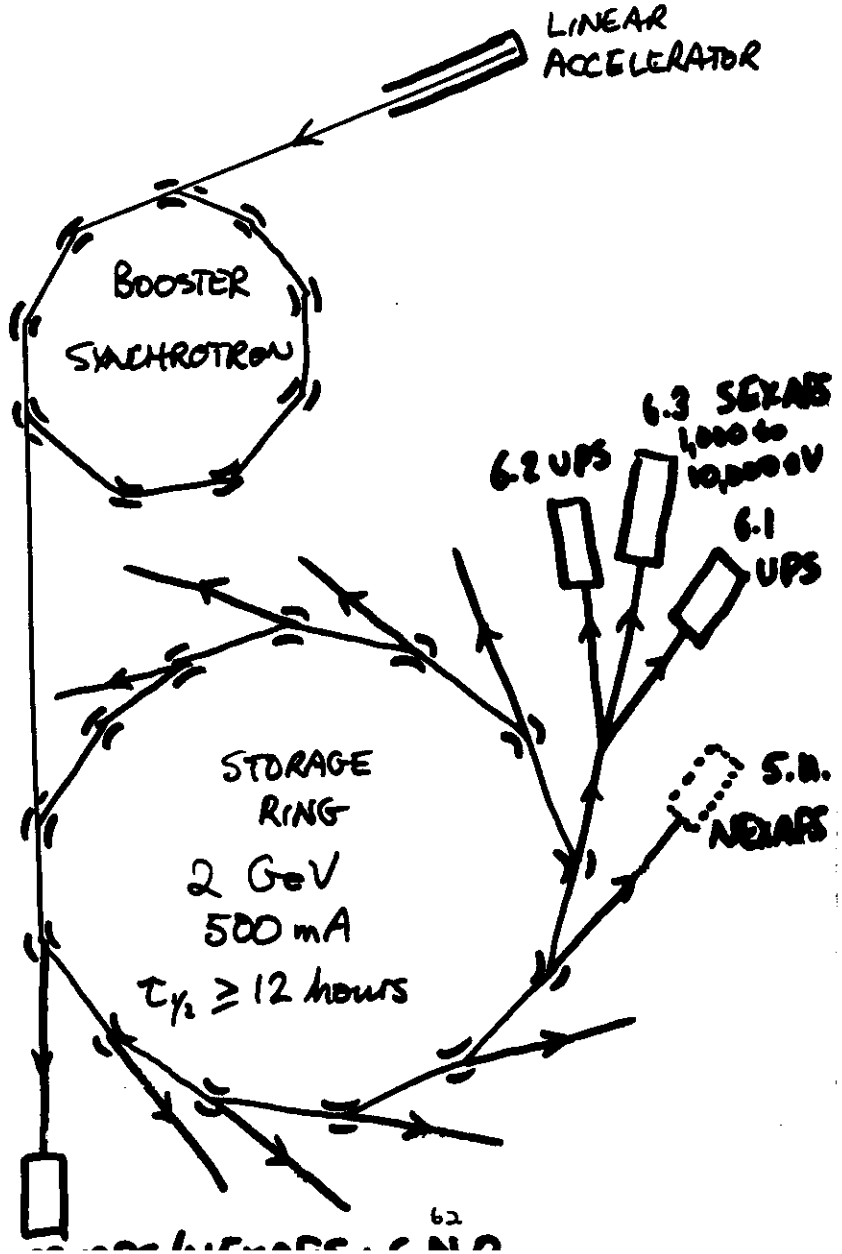

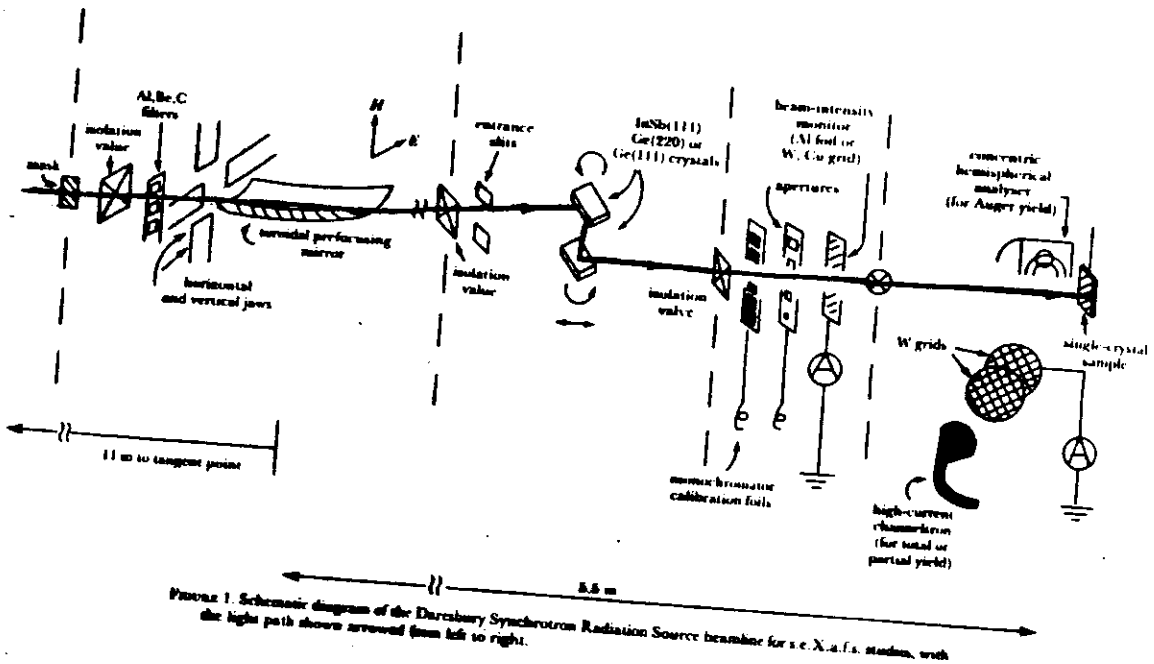

FIGURE 1. Schematic diagram of the Daresbury Synchrotron Radiation Source beamline for s.e.X.a.f.s. studies, with the light path shown arrowed from left to right.

LAMBLE AND KING, PHIL TRANS ROY SOC A318 (1986) 203

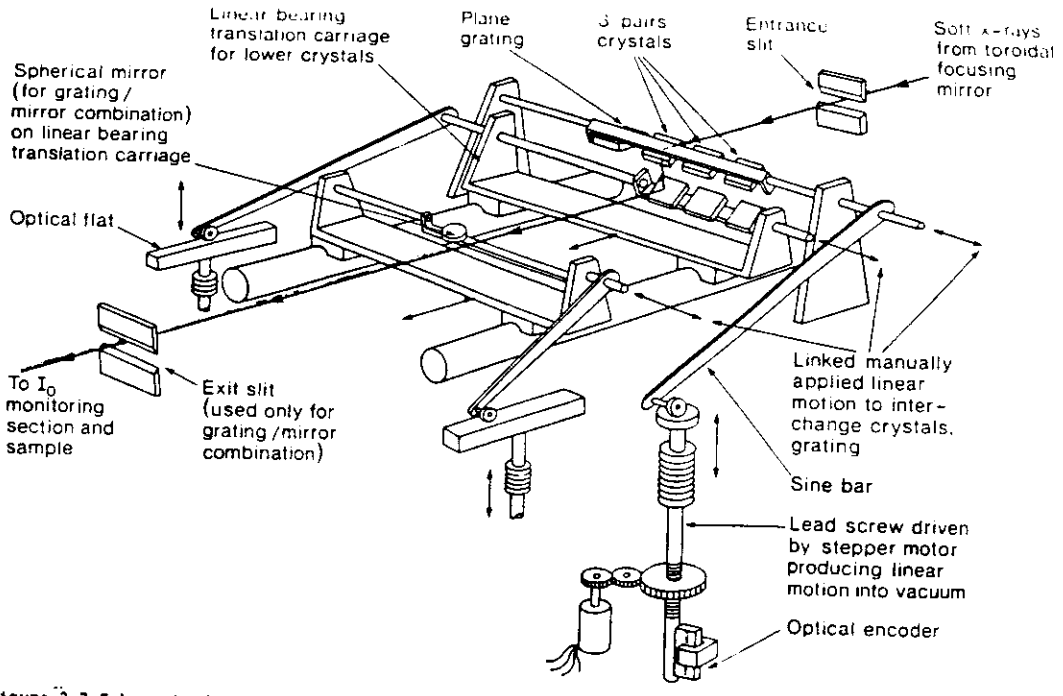

Figure 2.2 Schematic diagram of the soft X-ray monochromator used for SEXAFS studies on the Daresbury SRS beamline V.U.V. 6.3.

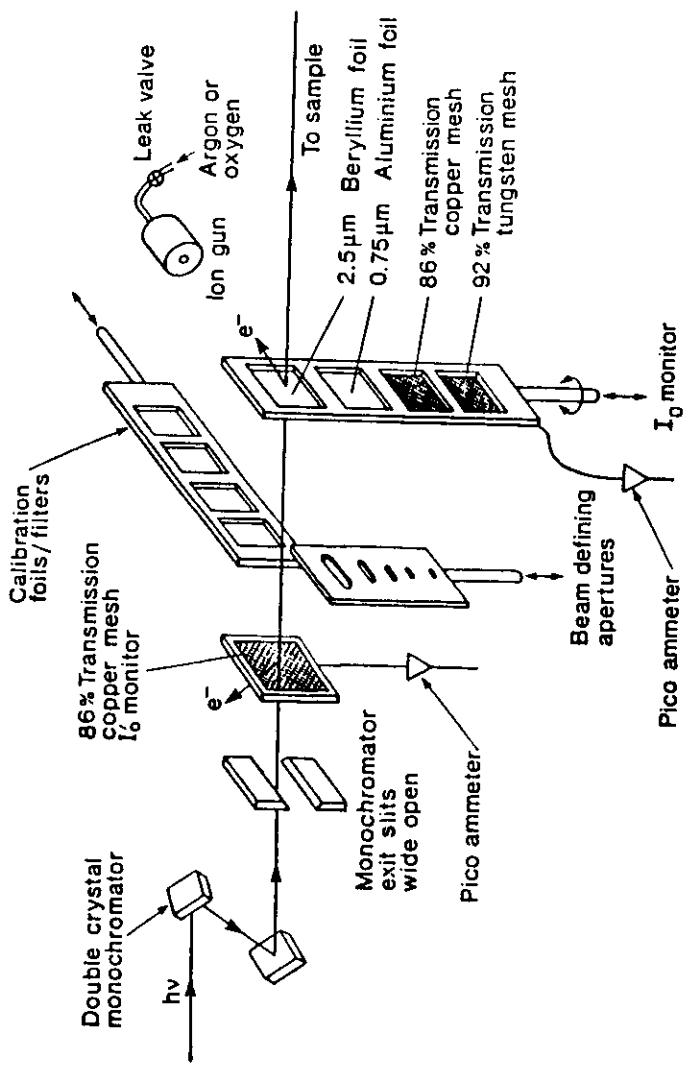

Figure 2.6 Schematic diagram of the beam intensity monitor manifold section, situated between the monochromator and the sample chamber.

ANALYTICAL PROCEDURES

1. Background subtraction and energy zero.

(a) Energy zero taken as point halfway up the absorption band edge, at photon energy E_0 .

(b) Background subtraction:

(i) Polynomial to fit pre-edge region to describe background absorption, μ_B.

(ii) Polynomial to fit post-edge region to describe the atomic-like absorption, μ_0.

2. Extraction of R_j from $\chi(k)$.

Two procedures used:

(a) The fourier transform method.

Widely used in EXAFS analysis. (KINEMATIC)

Used by all other groups in SEXAFS analysis.

(i) Bulk analogue compound EXAFS obtained.

e.g. NiI_2 for study of I on Ni (100).

(ii) Fourier transform of analogue and surface EXAFS spectra obtained; nearest neighbour peak windowed and back-transformed. Difference in phase of back-transformed spectra yields change in R_1,

i.e. $\Delta R = (R_1)_{bulk} - (R_1)_{surface}$.

(b) Curve fitting techniques.

Phase shifts, (e.g. MUFPOT), backscattering factors, σ_j^2, λ calculated.

$\chi(k)$ calculated for trial structures and compared with experimental $\chi(k)$ using reliability factors.

BOTH METHODS assume that MULTIPLE SCATTERING can be ignored: Pendry and Gurman, 1976.

● Combination method. (Used in this work.)

(i) Initial theoretical calculation of $\phi(k)$

(ii) Use of analogue compound structure with 3 to 5 shells to modify the calculated phase shifts until theory and experiment agree in $\chi(k)$.

(iii) Comparative cross-checking of phase shifts by interchanging between several model compounds.

(iv) Unknown surface structure varied with 1 to 5 shells to optimise the fit of the calculated and experimental SEXAFS spectra.

Fourier transforms used to improve comparisons.

Program based on theory of Lee and Pendry (1975); Rapid version: Binsted and Gurman (1984).

Example: Chlorine absorber and backscatterer phaseshifts interchanged between AgCl and CsCl gives error in nearest neighbour shell R_1 of $\lesssim 0.01$Å.

(Both Ag L_I and Cl K edges in AgCl examined.)
Important to allow E_0 and R_1 to vary independently to obtain good interchangeability.

Fig. 2

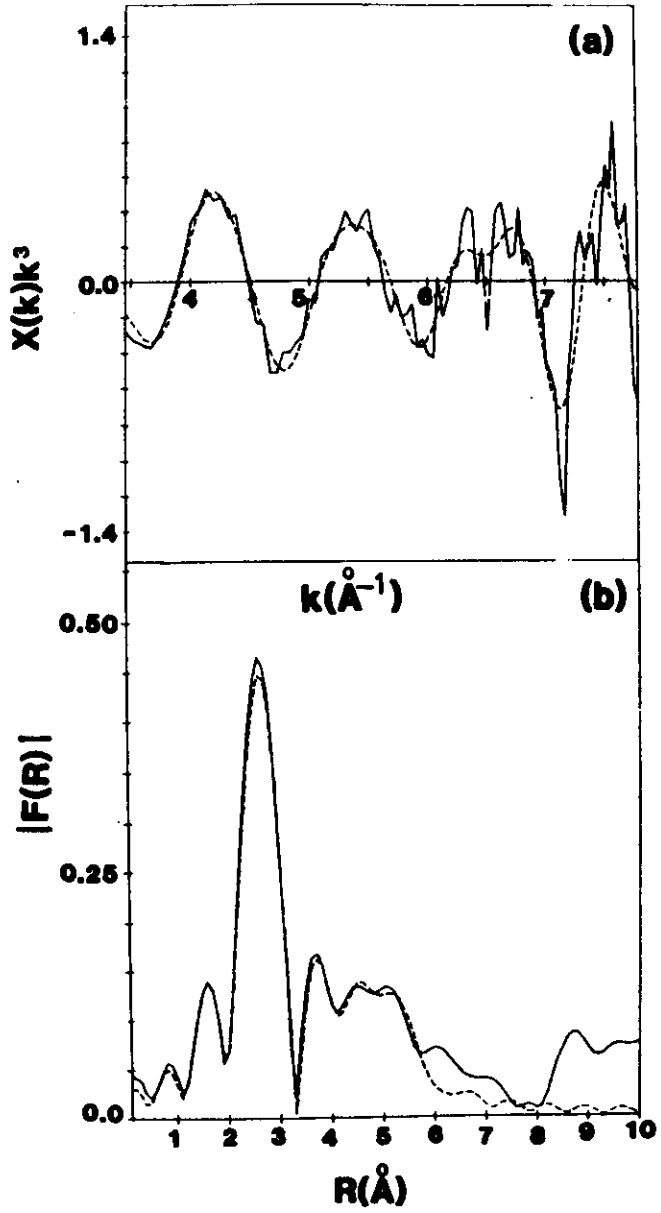

ATOMIC ADSORBATES.

CHLORINE ON AG(111).

(Chlorine used industrially to enhance selectivity of ethylene epoxidation reaction:

$$C_2H_4 \xrightarrow[O_2]{Ag} CO_2 + H_2C$$

$$C_2H_4 \xrightarrow[O_2]{Ag+Cl} C_2H_4O.\ )$$

LEED + TPD study: (Bonzel + Waugh 1984)

AT $\theta \simeq 0.7$ monolayer,

VERY DIFFUSE $(\sqrt{3} \times \sqrt{3})R30°$.

Mixed Layer Model suggested.

Quantitative Multishell analysis of SEXAFS data obtained at 100 K from Cl/Ag(111) at (disordered): $\theta = 0.35$ and $(\sqrt{3} \times \sqrt{3})R30°$: $\theta = 0.70$.

Phase shift transferability, anharmonicities, from bulk AgCl, AgBr, CsCl, KCl, etc.

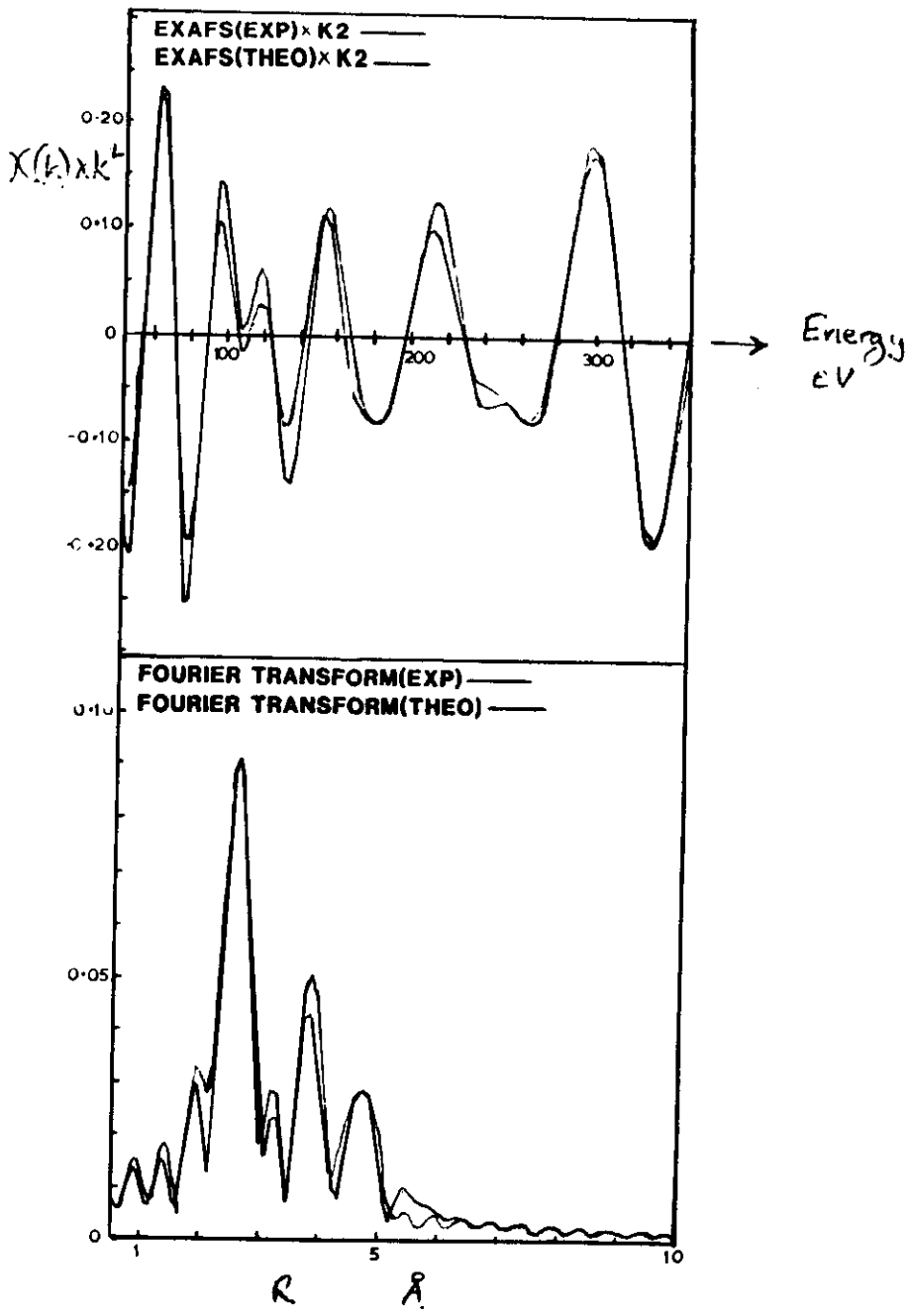

Cl K edge at 2870 eV

Cl/Ag (111) 0.7 ML COOLED

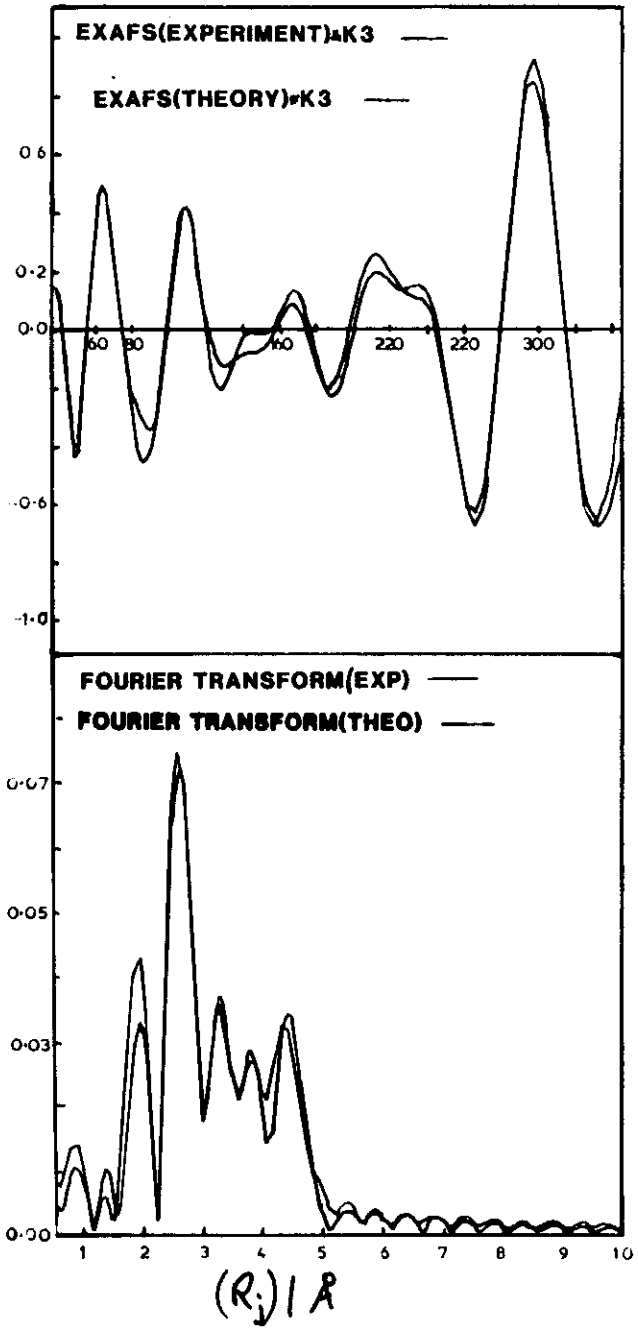

Cl/Ag {111} $\theta = 0.7$

$(\sqrt{3} \times \sqrt{3})R30°$ structure.

Shell	Number of neighbours Ni	Model Bond Distance Ri (Å)	Experiment Bond distance Ri (Å)
1. Cl-Ag	3	2·70	2·70
2. Cl-Cl	3	2·88	**2·93**
3. Cl-Ag	3	3·94	**3·71**
4. Cl-Cl	6	4·99	**4·33**

$\theta = 0.4$

1. Cl-Ag	3	2·70	2·70
2. Cl-Ag	3	3·93	**3·68**
3. Cl-Cl	6	4·99	**5·14**

SEE MODEL FORMAT LEED + AUGER

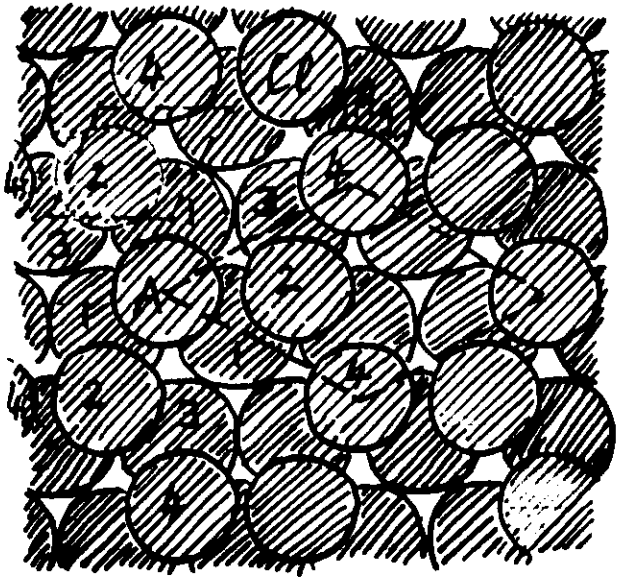

Ag {111}

$(\sqrt{3} \times \sqrt{3})R30° - Cl$

"Vacancy" structure:
HONEYCOMB MODEL

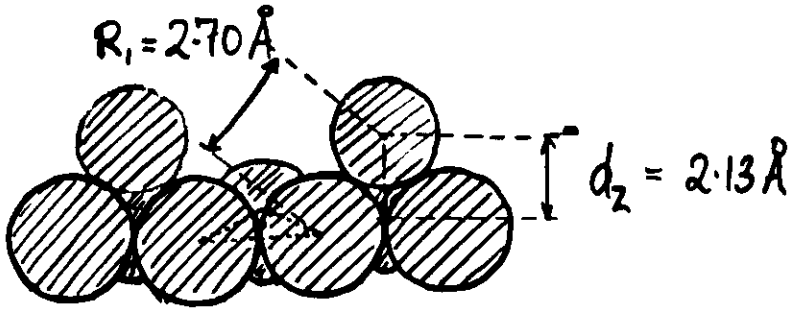

CHECKERBOARD MODEL OK!

$R_{Cl-Ag} = 2.70 Å \pm 0.01$

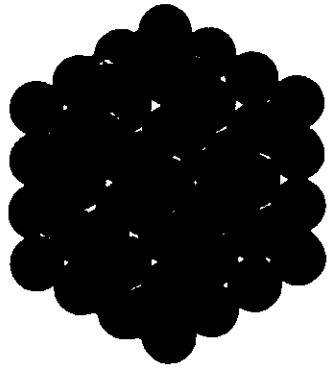

$R_{Cl-Ag} = 2.70 Å \pm 0.01$

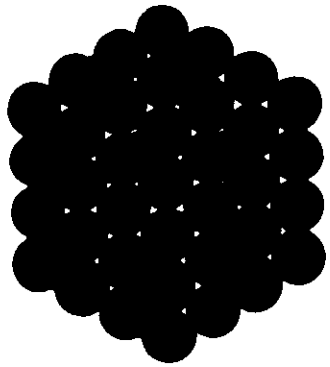

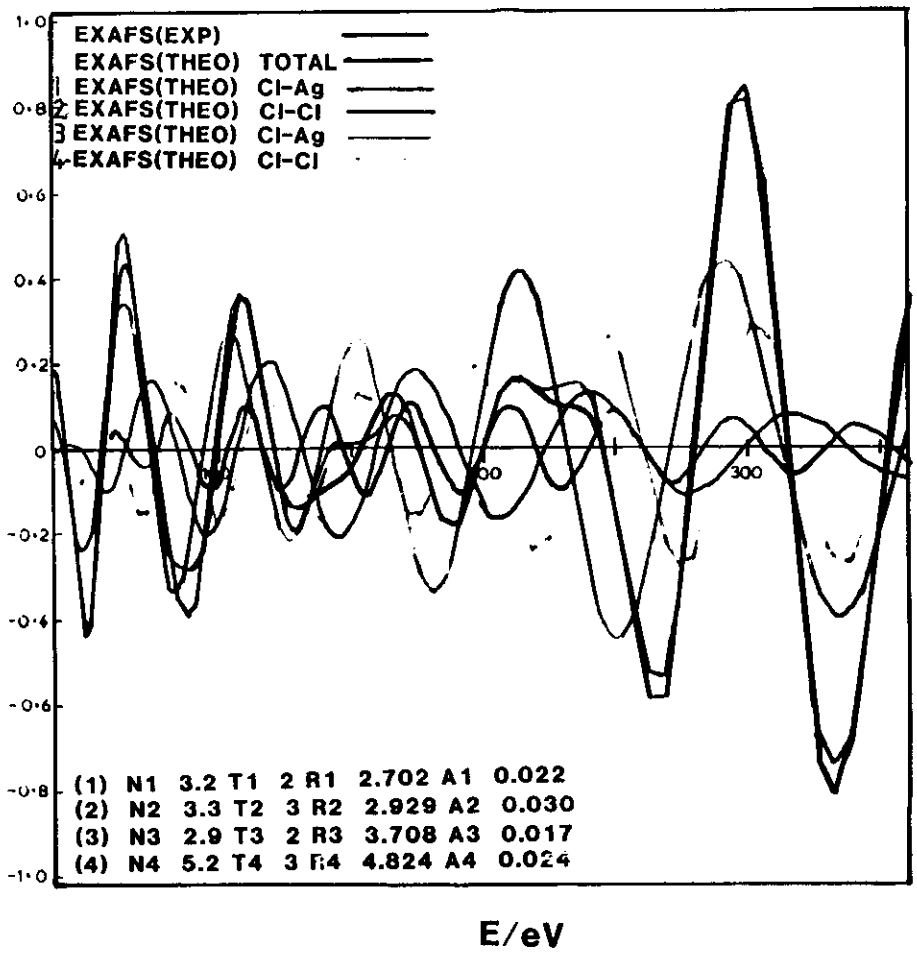

POLARIZATION DEPENDENCE IN SEXAFS.

normal incidence

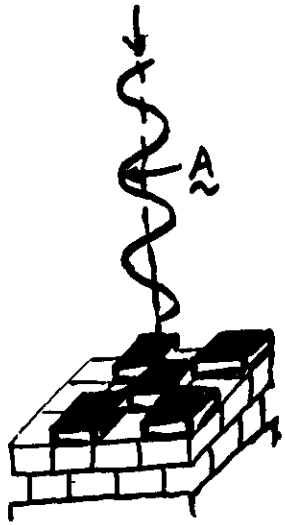

SENSITIVITY TO ATOMIC SHELLS IN SURFACE PLANE

grazing incidence.

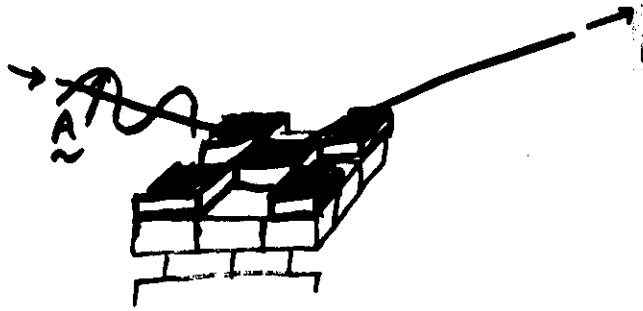

SENSITIVITY TO ATOMIC SHELLS ⊥AR TO SURFACE PLANE.

STRUCTURE DETERMINATION BY SEXAFS*: CHLORINE ON SILVER {110}.

HOLMES, PANAGIOTIDES, DUS, NORMAN, LAMBLE, DELLA VALLE AND KING

[illegible] UNIVERSITY

(DARESBURY SRS)

SPECIFIC PROBLEM:

LEED UNABLE TO DISTINGUISH A UNIFORMLY INCOMMENSURATE STRUCTURE FROM A DOMAIN WALL (SOLITON) STRUCTURE.

SEXAFS PROBES LOCAL STRUCTURE. CAN IT REMOVE THE AMBIGUITY?

Cl/Ag{110} at $\theta = 0.75$ MONOLAYERS, LEED SHOWS INCOMMENSURATE STRUCTURE

*SURFACE EXTENDED X-RAY ABSORPTION FINE STRUCTURE

Fig. 3(a) Cl/Ag{110}, $\theta = 0.75$

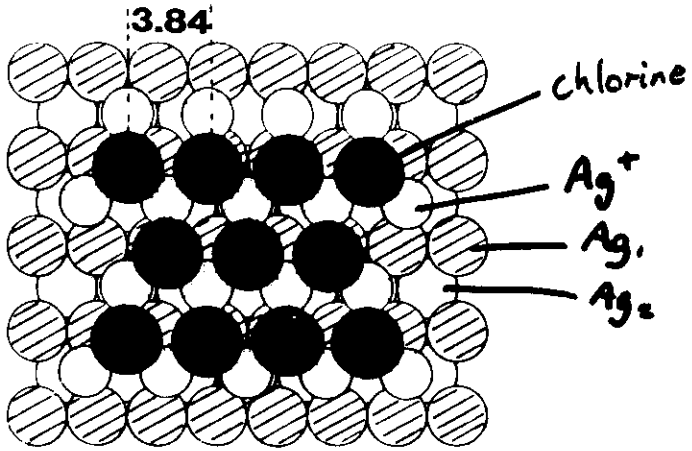

Rowe & Pratesi: mixed layer model

Fig. 3(b)

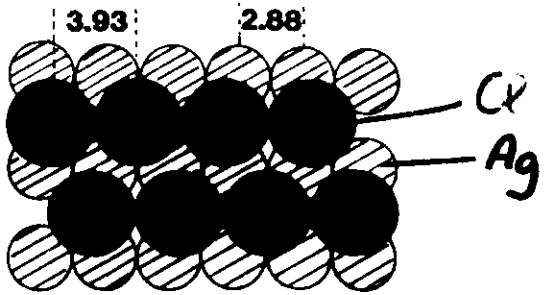

Bowke- and Waugh: fully (uniformly) incommensurate overlayer model.

SEXAFS ANALYSIS : Cl/Ag(111)

Run	$\vec{A}$	r_1 (Ag)	r_2 (Cl)	r_3 (Ag)	r_{11} (Cl)
1	⟨100⟩	2.57 Å	3.19	3.49	3.86
2		2.57	3.19	–	4.11
3		2.56	3.11	3.62	4.05
4		2.54	3.11	3.54	–
5		2.60	3.11	–	4.11
6		2.55	3.18	3.51	4.09
7		2.58	3.18	–	4.12
MEAN	⟨100⟩	2.57±0.03	3.14±0.04	3.46±0.06	4.05±0.03
8	⟨110⟩	2.56	3.20	3.44	4.11
9		2.56	3.12	–	–
10		2.62	3.16	3.58	–
11		2.58	3.20	–	3.98
12		2.53	3.01	3.44	4.16
13		2.55	3.16	3.44	4.07
14		2.52	3.19	3.40	4.04
MEAN	⟨110⟩	2.56±0.03	3.14±0.04	3.46±0.06	4.09±0.07

Fig. 3(c)

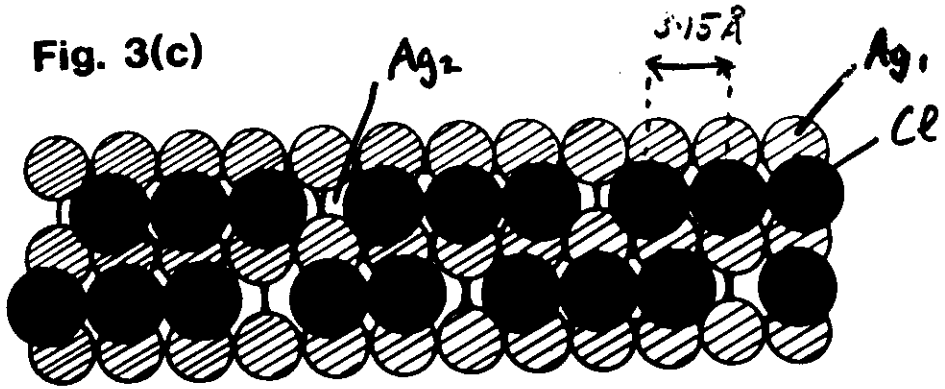

Vacancy domain wall model: linear chains, long bridge site

Fig.3(d)

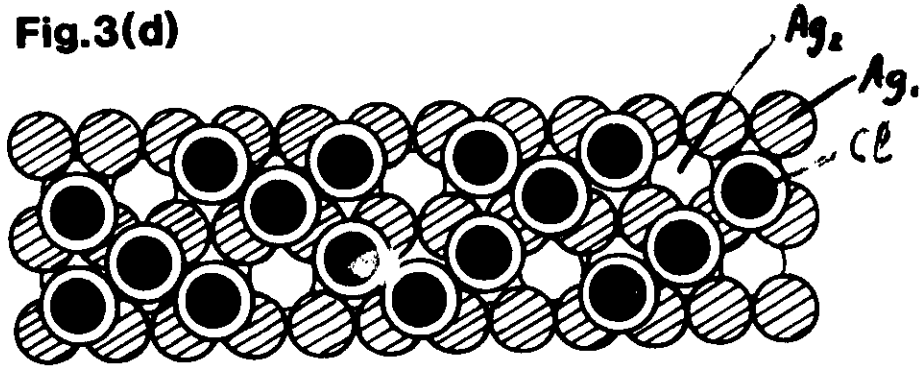

Vacancy domain wall model, sig-zag chains, '3-fold' coordination site.

Linear simulation: [illegible] both domain wall [illegible] ye[illegible] observed [illegible] (1/4 ½)

Fig 4(a)

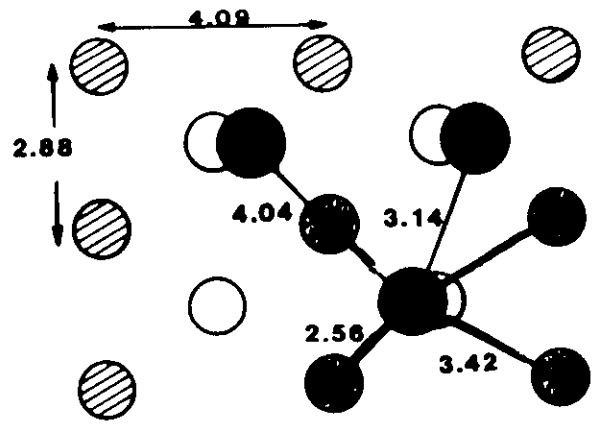

Plan view, vacancy domain wall model, zig-zag chains.

Fig 4(b)

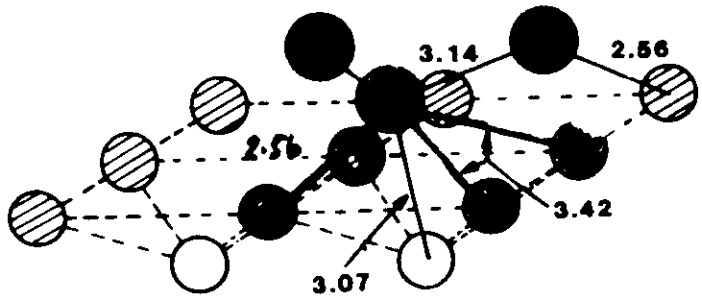

Isometric projection

RELIABILITY OF SEXAFS FOR DETERMINING ATOMIC LOCATIONS AT SURFACES

COLLABORATORS:
DANNY HOLMES
DAVE BATCHELOR

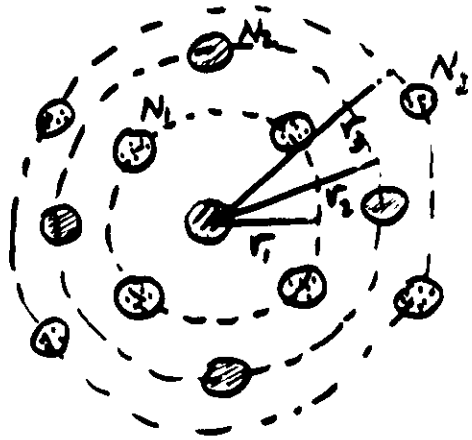

HOW ACCURATE/RELIABLE ARE

$r_1, r_2, r_3, \ldots r_j$

$N_1, N_2, N_3, \ldots N_j$. ?

MEAN VALUES OF r_j, N_j^{eff} AND A_j OBTAINED FROM 10 INDEPENDENT ANALYSES OF SIMULATED SENSE DATA:

r_j/A

	INPUT	OUTPUT (100)	OUTPUT (110)
j=1 (A_1)	2.50	2.55 ± 0.01	2.50 ± 0.01
j=2 (A_2)	3.14	3.11 ± 0.04	3.22 ± 0.09
j=3 (A_3)	3.61	3.46 ± 0.01	3.67 ± 0.03
j=4 (C)	4.05	4.05 ± 0.08	4.03 ± 0.02

N_j^{eff}

	INPUT	OUTPUT (100)	IN OUTPUT (110)	
j=1 (A_1)	1.9	2.1 ± 0.2	1.9	2.1 ± 0.2
j=2 (A_2)	0.6	2.1 ± 0.6	3.4	2.2 ± 2.1
j=3 (A_3)	3.7	1.8 ± 0.6	1.1	4.1 ± 1.8
j=4 (C)	2.0	4.1 ± 1.6	2.0	3.1 ± 1.1

A_j [illegible] λ^2

	INPUT	[illegible]	[illegible]
j=1 (A_1)	0.02	[illegible] ± 0.003	[illegible]
j=2 (A_2)	0.05	[illegible] ± 0.001	[illegible]
j=3 (A_3)	0.02	[illegible]	[illegible]
j=4 (C)	0.05	[illegible]	0.036 ± 0.013

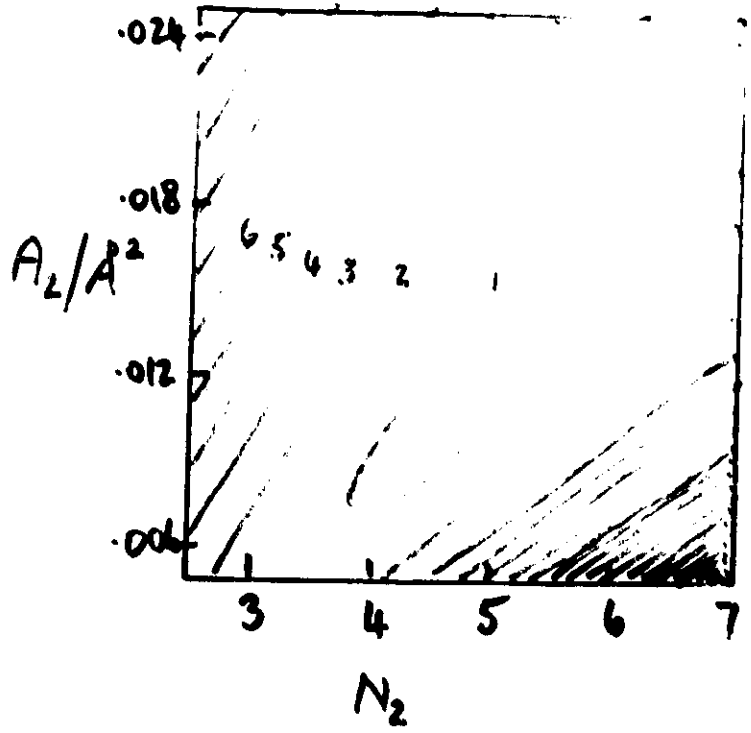

INTERCORRELATIONS IF CRITERION COORDINATE N_j AND INTERCEPT TERM A_j.

FROM THIS CONTOUR PLOT, STATISTICAL ANALYSIS YIELDS

$$N_2 = 5.5 \pm 3$$

CONCLUDE:

FOR SEXAFS DATA TAKEN AT LOW TEMPERATURE (~ 100 K):

1.) FIRST SHELL SPACING r_1 TO 0.01 Å

2.) FIRST SHELL COORDN. N_1 TO ± 0.2.

3.) SPACINGS REPRODUCED &c.
FOUR SHELLS TO BETTER THAN 0.04 Å.

4.) SHELLS SEPARATED BY ≥ 0.3 Å ARE DISTINGUISHED.

5.) COORDINATION NUMBERS OF HIGHER SHELLS UNRELIABLE, AS HIGH AS ± 3.

COVERAGE DEPENDENCE OF ADSORBATE – SUBSTRATE BOND LENGTH.

1.) CHLORINE – SILVER.

PLANE	θ	SITE	$d_{Ag\text{-}Cl}$
BULK AgCl			2.77 Å
{111}	0.4	○○○	2.70
	0.7	○○○	2.70
{110}	0.4	○○○○	2.56
	0.75	○○○○	2.56

2.) CAESIUM – SILVER

{111}	0.2	○○○	3.20
	0.4	○○○	3.50 (SATD FIRST LAYER)

CRYSTAL PLANE DEPENDENCE

CHLORINE – SILVER

{111}	2.70 Å
{100}	2.69
{110}	2.56

SURFACE CORE LEVEL SHIFTS.

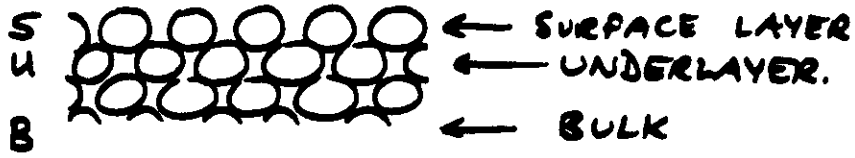

AT VERY HIGH RESOLUTION (~150 meV) IT IS FOUND THAT THE ELECTRONIC CORE LEVEL BINDING ENERGIES FOR SURFACE LAYER ATOMS (S) ARE SHIFTED W.R.T. BULK ATOMS (B)

- HIGHER BINDING ENERGY: Ta, Gd, Yb
  $< \frac{1}{2}$ filled d-shell
- LOWER BINDING ENERGY: W, Ir, Au
  $> \frac{1}{2}$ filled d-shell.

EXPLANATION:

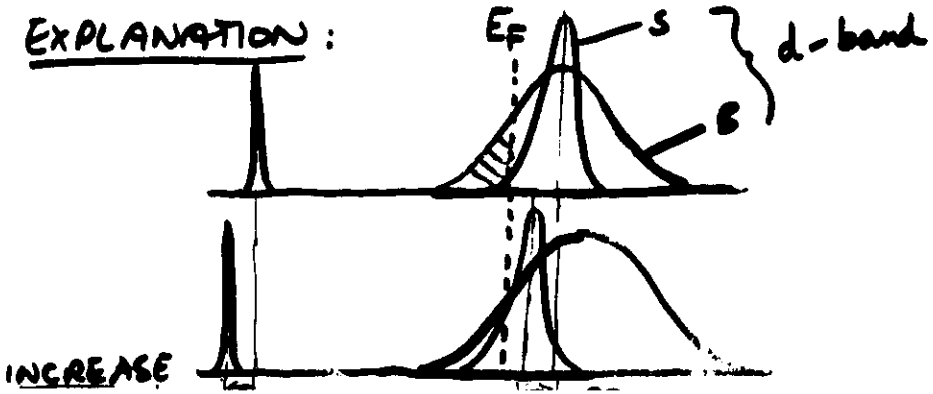

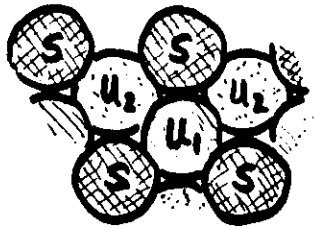

$h\nu = 75eV$

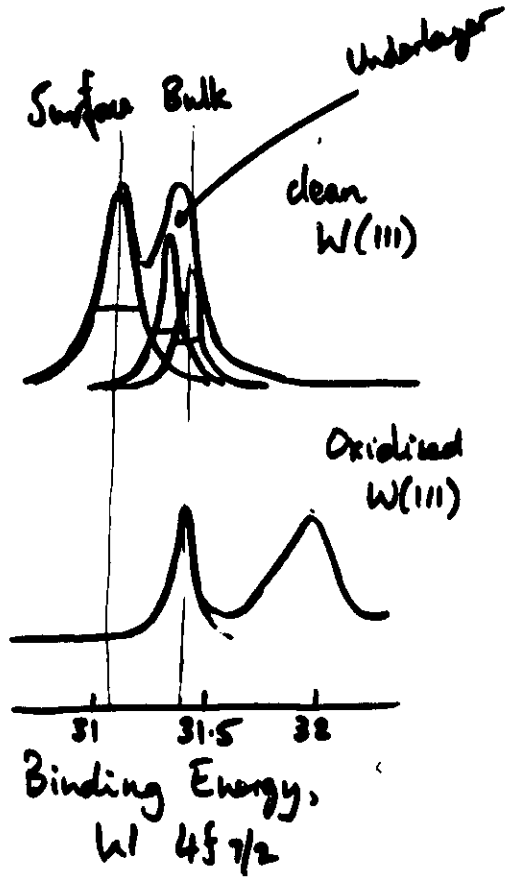

OXIDISED W{111}

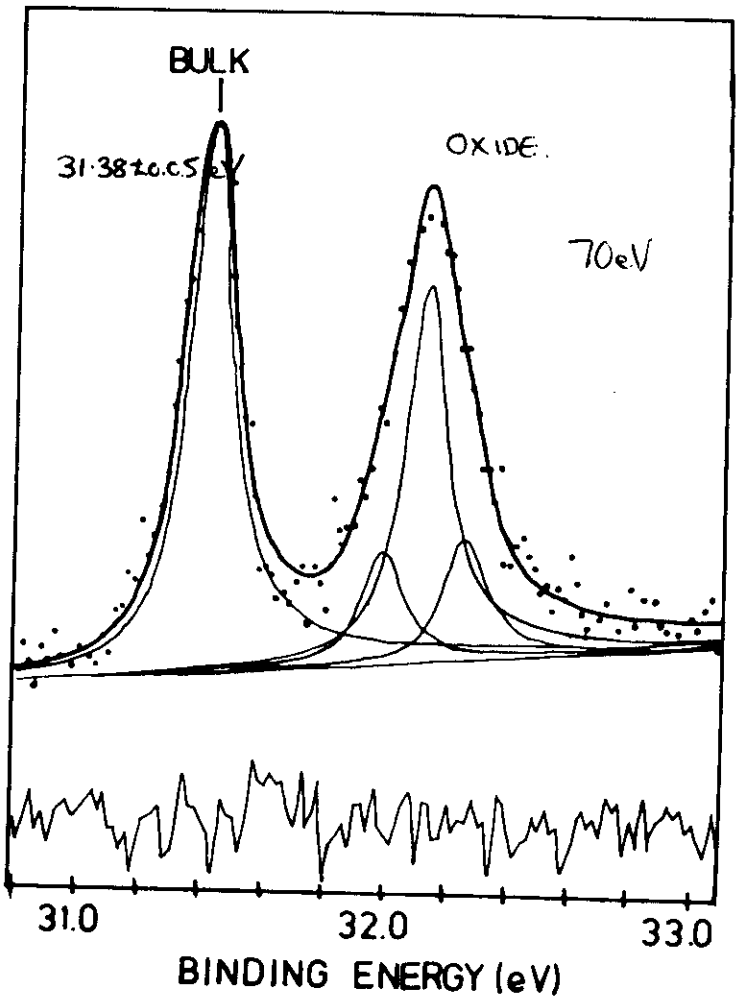

LINESHAPE

DONIACH - SUNJIC FWHM = 0.15eV

α = 0.05

CONVOLVED WITH A GAUSSIAN

INSTRUMENT FUNCTION FWHM = 0.16eV

W(111) : 4-peak fitting.

W4f-7/2 Core Level Shifts:

S : 460 meV

U_1 : 360 meV

U_2 : 110 meV.

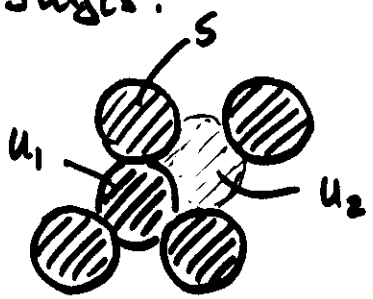

Dependence of Core Level Shift on Coordination Number.

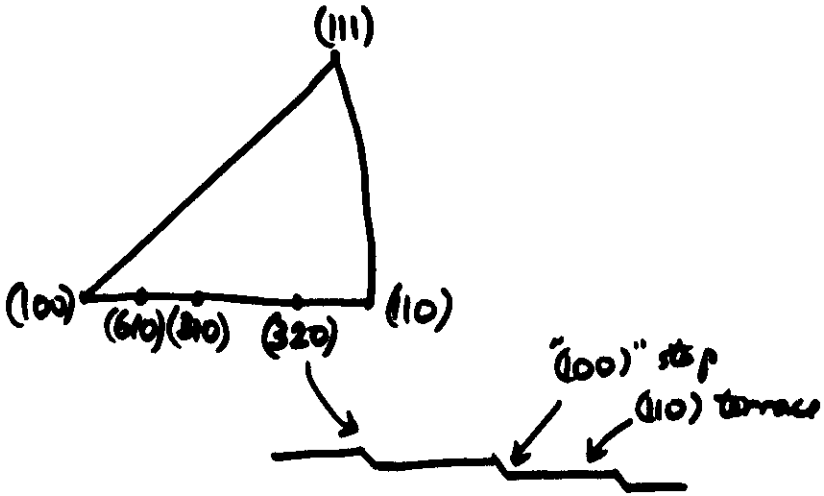

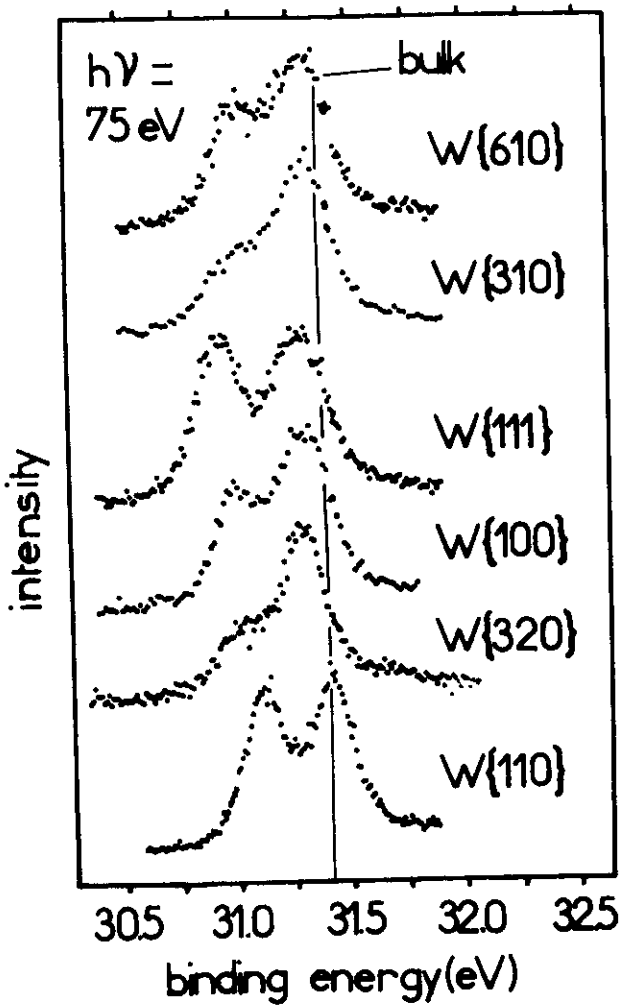

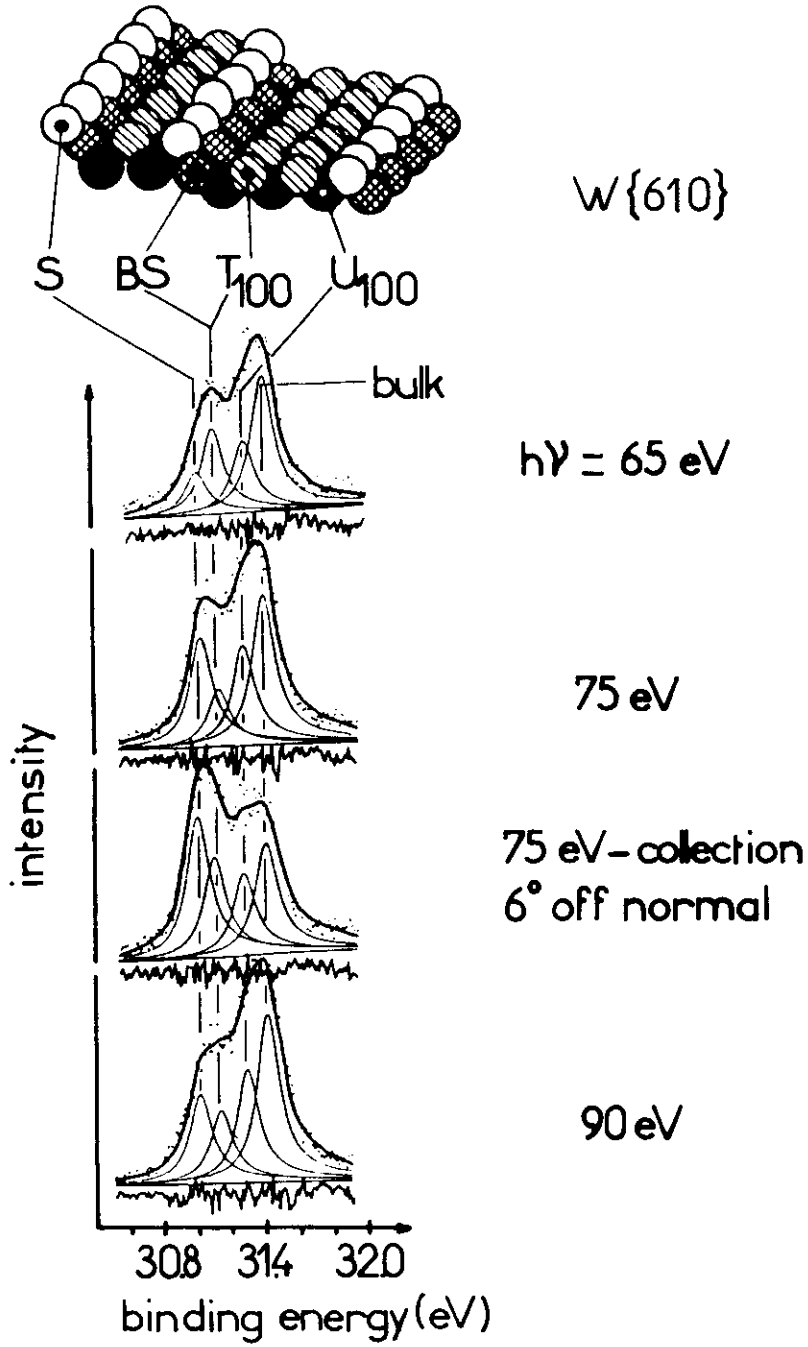
S
BS
T100
U100
bulk
W{610}
hν = 65 eV
75 eV
75 eV-collection
6° off normal
90 eV
intensity
30.8
31.4
32.0
binding energy(eV)

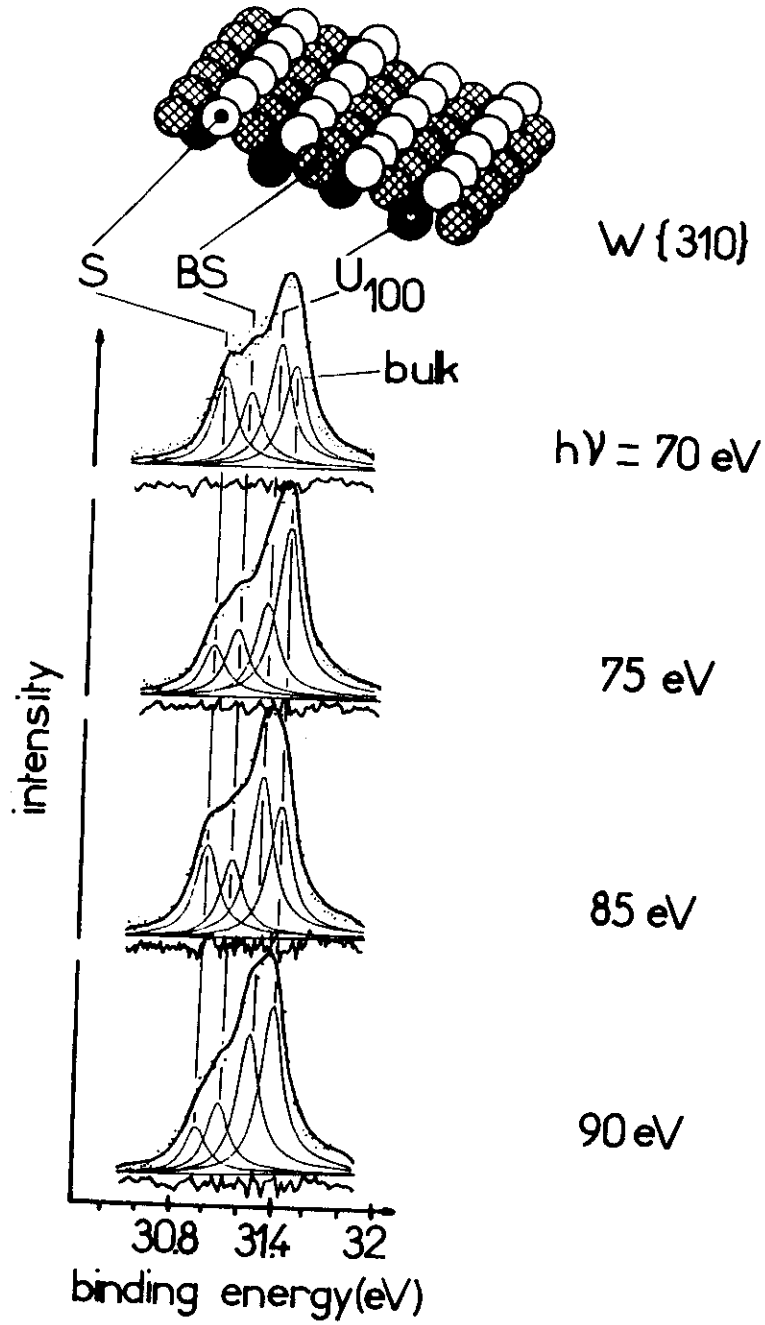
S
BS
U100
bulk
W{310}
hν = 70 eV
75 eV
85 eV
90 eV
intensity
30.8
31.4
32
binding energy(eV)

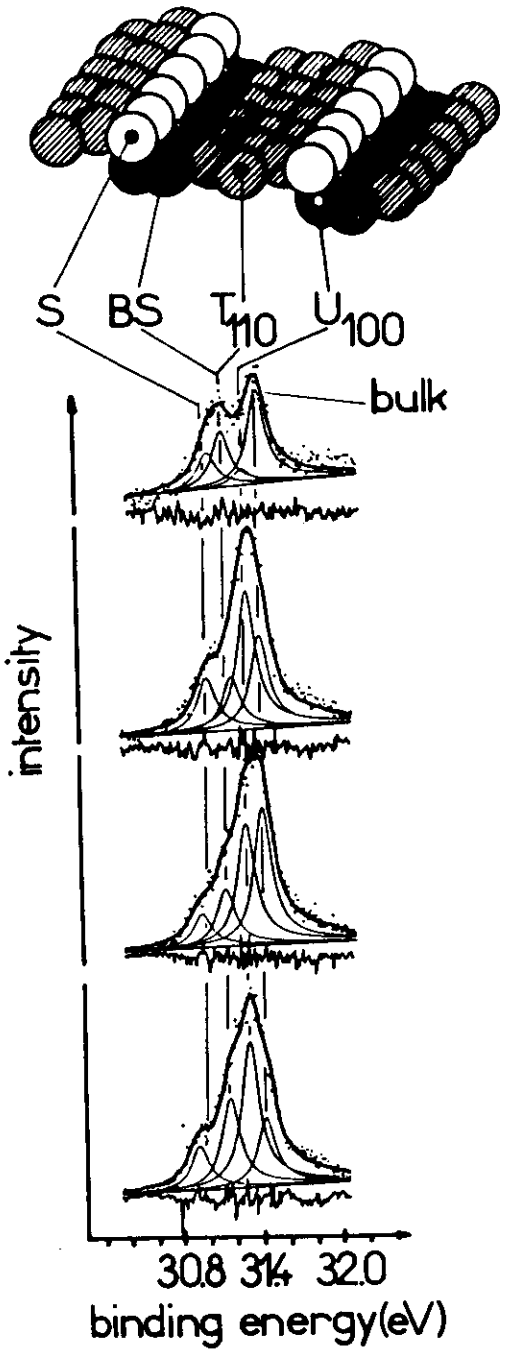

W{320}

hν = 60 eV

70 eV

85 eV

90 eV

Comparison of Core Level Shifts from the same Coordination Site on different surfaces.

Shifts in meV

Site type	Coord.	W(320)	W(310)	W(610)
S_{step}	4,4	-410 meV	-430	-380
S_{100}	4,5			-380
S_{110}	6,4	-250		
S_{base}	6,5	-250	-290	-280
S_u	8 5	-100	-120	-120

	W(111)	W(100)	W(110)
4,3	-430		
4,5		-360	
6,4			-280
7,3	-210		
7,6	-110		

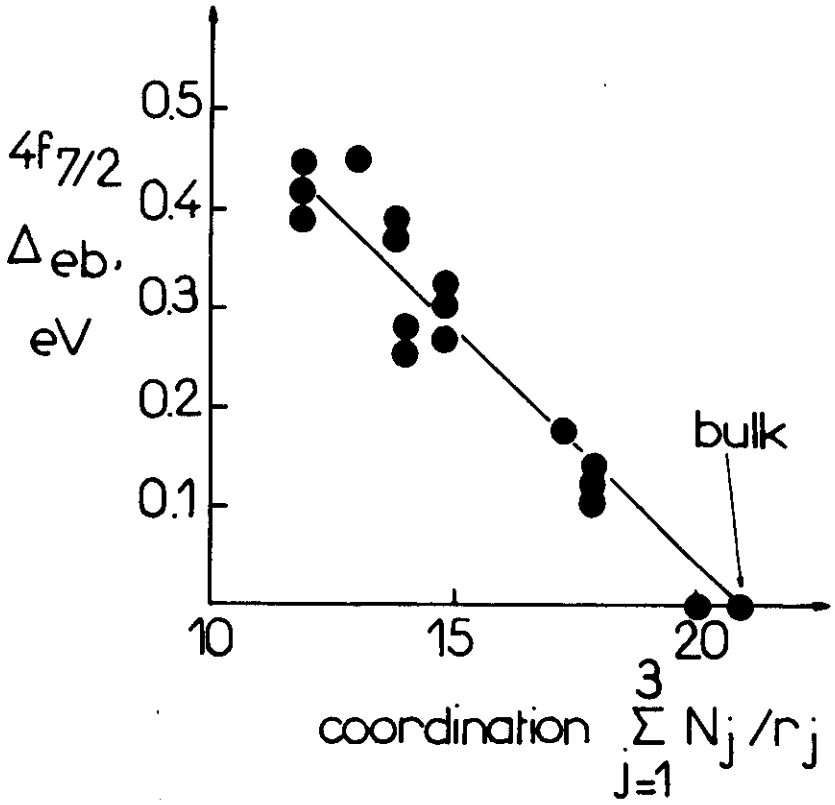

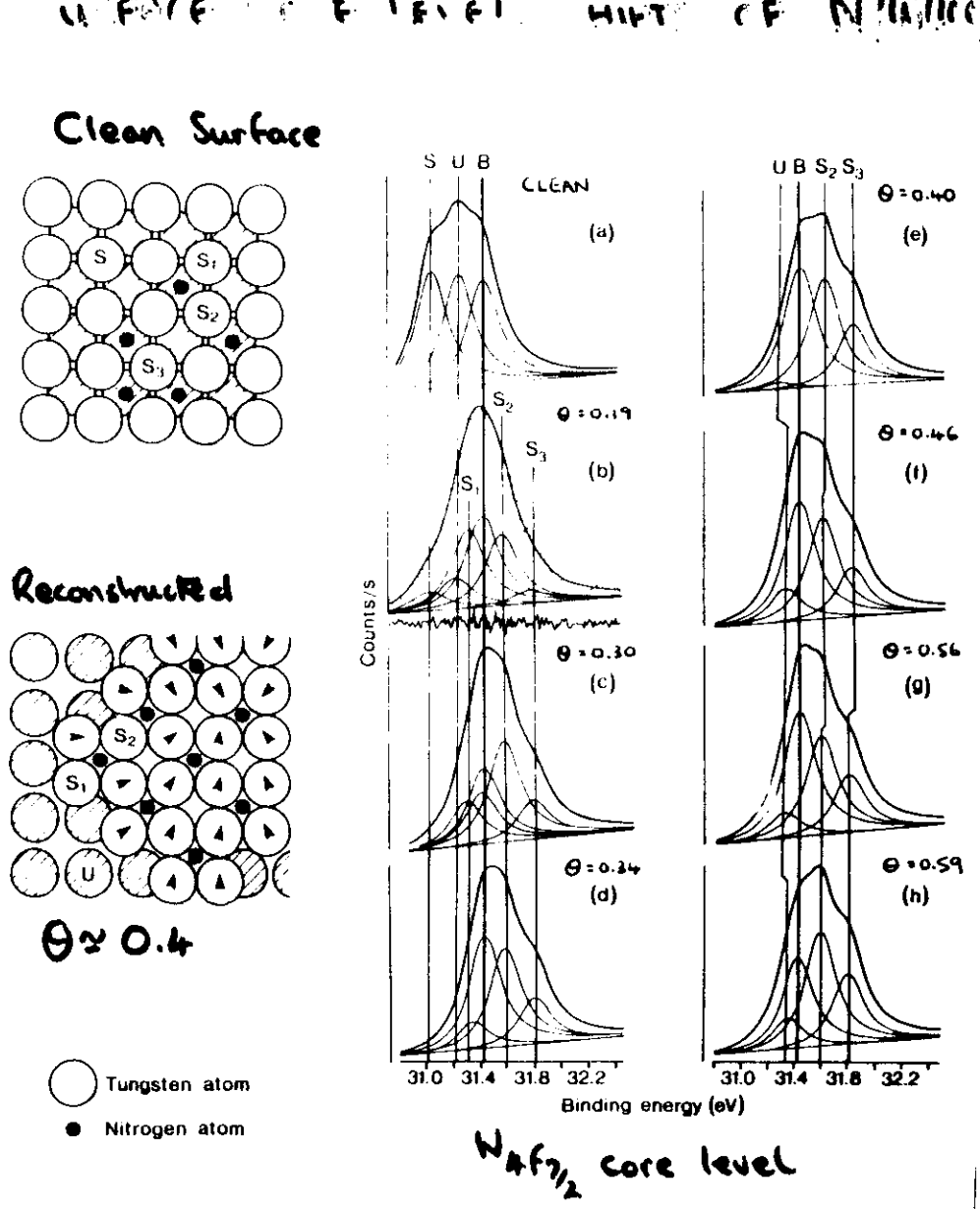

$N_{4f_{7/2}}$ core level

Determination of phonon broadening on W 4f7/2, W(110)

Natural linewidth: (Doniach-Sunjic)
50 meV, lifetime broadening.

Measured Gaussian linewidth Γ_G:

Temp./K	CLS (meV)	Γ_G (meV)	Γ_{phonon} (meV)
100	-290 meV	175	71
290	-290	185	92

(Measured instrum contribution to Γ_G: 162 meV.)

Theoretical measurement:
Sebilleau: 100 K, Γ_{ph} = 70 meV
300 K, Γ_{ph} = 90 meV

Work function changes:

1.) alkali metal adsorption on metals

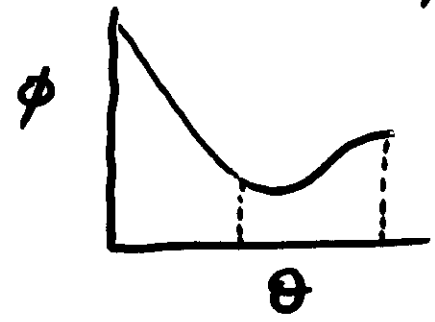

2.) chlorine adsorption: no reconstruction.